DOE/CE/40992--T1

Submitted: April 7, 1998

To: U.S. Department of Energy
Chicago Operations Office
9800 South Cass Avenue
Argonne, IL 60434
Attn: Jill Jonkouski

FINAL REPORT SUBMITTED TO THE DEPARTMENT OF ENERGY

By

The Dow Chemical Company
1776 Building
Midland, MI 48674-1776

For

CONTINUOUS FIBER CERAMIC COMPOSITES FOR ENERGY RELATED APPLICATIONS

Cooperative Agreement
DE-FC02-92CE40992

DISCLAIMER

EXECUTIVE SUMMARY

The U.S. Department of Energy has established the Continuous Fiber Ceramic Composites (CFCC) program to develop technology for the manufacture of CFCC's for use in industrial applications where a reduction in energy usage or emissions could be realized. As part of this program, the Dow Chemical Company explored the manufacture of a fiber reinforced/self reinforced silicon nitride for use in industrial chemical processing. In Dow's program, CFCC manufacturing technology was developed around traditional, cost effective, tape casting routes. Formulations were developed and coupled with unique processing procedures which enabled the manufacture of tubular green laminates of the dimension needed for the application. An evaluation of the effect of various fibers and fiber coatings on the properties of a fiber reinforced composites was also conducted. Results indicated that fiber coatings could provide composites exhibiting non-catastrophic failure and substantially improved toughness. However, an evaluation of these materials in industrial process environments showed that the material system chosen by Dow did not provide the required performance improvements to make replacement of current metallic components with CFCC components economically viable.

I. INTRODUCTION

The Dow Chemical Company has conducted this research and development program as a first of three phases of the U.S. Department of Energy's Continuous Fiber Ceramic Composites (CFCC) Program. This work has been completed under cooperative agreement # DE-FC02-92CE40992.

The overall objective of this program was to develop processes which can be used to manufacture fiber-reinforced/self reinforced silicon nitride (SRSN) composite materials. These materials may be useful in physically demanding, high temperature applications such as those needed to improve the energy efficiency and reduce the emissions from industrial equipment. Specifically, in Phase I of this program, The Dow Chemical Company, hereafter referred to as Dow, targeted cracking tubes used in the production of ethylene as the application to guide the development of it's CFCC technology.

The critical technical issues addressed in this program were:

- The energy impact of the use of CFCC's reactor tubes in the production of ethylene.
- The economics of the tape casting process relative to the value of the final components.
- The optimization of the tape casting formulations and development of processes for utilizing tapes to manufacture tubular shapes.
- The exploration of densification routes for composites.
- The evaluation of candidate fibers and fiber coatings.
- The compatibility of composites with application process environments.

Dow's Statement of Work for the technical tasks of this program can be found in its entirety in Appendix A. Each of the issues described above will be discussed in detail in the sections to follow.

II. ENERGY IMPACT AND ECONOMICS

A. Assessment of Energy Impact

A preliminary energy impact study was conducted in the early stages of this program to determine what the effect of using a CFCC would be on the energy consumption during the production of ethylene in a typical cracking operation. In the production of ethylene, ethane is converted to ethylene using a steam cracking furnace. During normal operation of this facility, formation and build-up of significant amounts of coke require that periodic burn outs of each furnace tube be conducted. At the time this study was conducted, the cost of removing the coke build-up in Dow facilities was estimated to be $2.35 MM per year. The original impetus for this work was to replace the metallic tubes currently being used with CFCC tubes that could potentially inhibit the coke forming reaction, while concurrently maintaining the mechanical integrity required for this application.

For the purposes of the energy impact study, it was assumed that use of a CFCC component would decrease the number of burn out cycles in this process by a factor of four. Based on this assumption, use of these CFCC's could potentially reduce the cost for coke removal by $1.76 MM per year for Dow facilities.

A reduction in energy consumption, and thus a reduction in operating costs, is an important part of Dow's goals. However, a dominating factor which dictates the success of CFCC's in any application is the cost/performance ratio. Performance requirements dictate that Dow's cracking tubes not only show reduced coke formation, but be capable of surviving for extended periods of time without failure. The cost to Dow for shutting down a plant to replace failed components is enormous, primarily due to down time and product losses from these high operating capacity plants. Extended component lifetime is therefore a critical factor. However, there are limitations on how much a component can cost for this to remain an economically viable solution. A low cost production route is therefore an integral part of Dow's CFCC development effort.

B. Process Economics

In Phase I, Dow explored a modified tape casting and lamination technique which will be described in more detail in later sections. To assess the potential cost of using this technique in the manufacturing of CFCC cracking tubes, an economic evaluation of this process was performed. Estimates on the plant size and number of components being manufactured were based on the potential market size. A more detailed description of these estimates can be found in Appendix B. Table I shows a breakdown of the cost of manufacturing tubular components for Dow's application. Clearly, the cost of these CFCC tubes is dominated by raw material costs. The process itself (labor, capital, etc...) represents a much smaller portion. In addition, as indicated in Figures 1 and 2, the raw material costs consist primarily of fibers and fiber coatings. This data includes estimated cost reductions for both fibers and fiber coatings based on increased volume usage. While these costs are extremely high, even with estimated cost reductions, the sensitivity to raw material cost allows for additional cost reductions should the cost of fibers and fiber coatings decrease beyond our estimates.

This study shows that the tape casting technique being developed under Phase I can be an inexpensive process and that the product cost is dependent primarily on the cost of the materials. Consequently, the cost/performance ratio will depend on the development of inexpensive fibers and fiber coating technology.

Of course, the composite manufacturing technology must be developed concurrently with cost reductions and stabilization of material supply lines. In Dow's program, we concentrated a majority of our efforts on technology development. Our program consisted of four major segments which fall under Task 3 of the CFCC program: 1) process development, 2) component fabrication, 3) densification, and 4) interfacial modification. Each of these segments is discussed in more detail below.

	Cost Estimate $/Tube	Capital Cost $/Unit/Yr
Fiber	60,442.67	0
Fiber Coatings	91,579.82	0
All Other Materials	13,590.02	0
Total R.M.	165,612.51	0
Labor, Utilities, Waste Disposal, Maintenance	9,659.23	0
Overhead, Depreciation, DFC,Taxes	6,020.08	34,646.95
R.M. Inventory	0	6,440.45
In-Process Inventory	0	1,209.57
Transfer Inventory	0	2,456.99
Total Bulk	181,291.84	45,753.96
Packaging	1,134.82	0
Total Plant	182,426.66	45,753.96
Selling, Gen. & Adm., Research, Cash & Acc.	20,751.30	37,862.21
Inventory for Sale	0	12,934.95
Total Cost per Tube	203,177.94	96,551.12
	203,177.94	95,551.12

Table I. Preliminary economics of manufacturing CFCC cracking tubes.

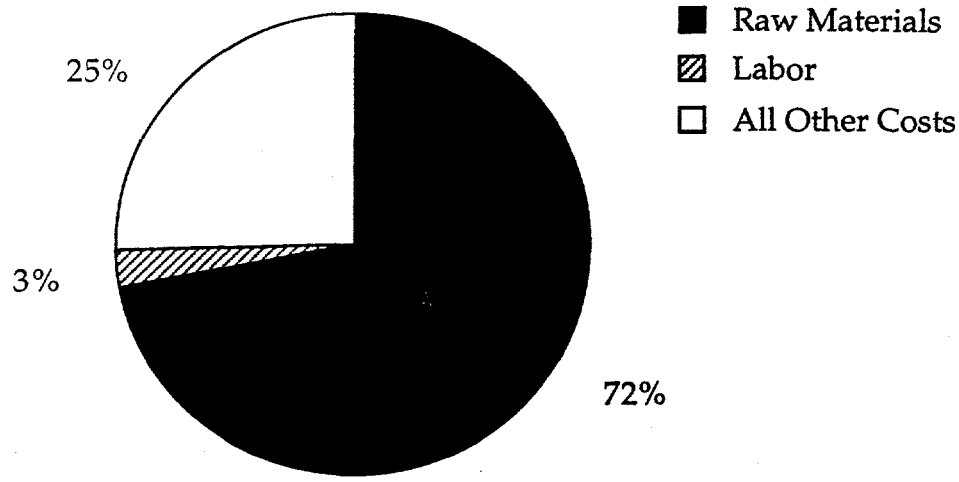

Figure 1. Cost breakdown for manufacture of CFCC ethylene cracking tube.

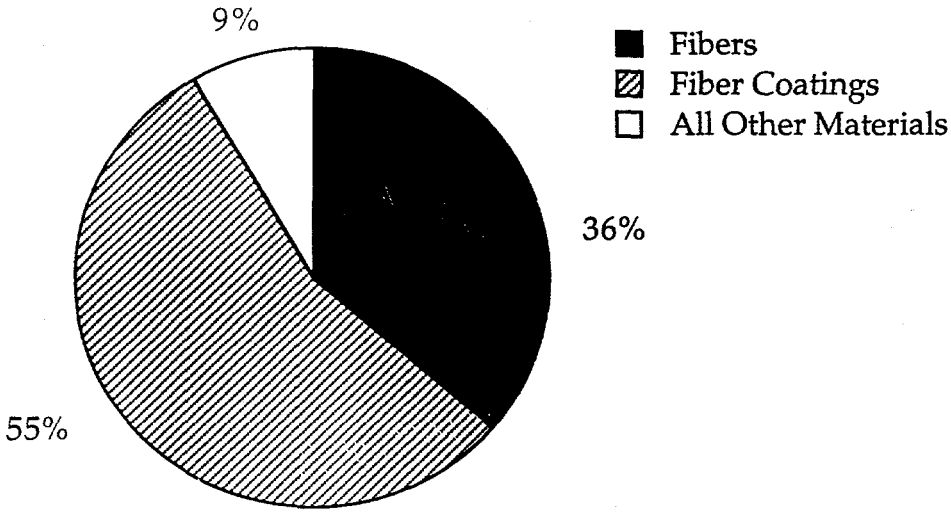

Figure 2. Breakdown of raw material costs for manufacture of CFCC ethylene cracking tube.

III. PROCESS DEVELOPMENT

A. Introduction

Numerous approaches to the manufacture of fiber composites have been explored over the years. These approaches include chemical vapor infiltration (CVI) (1-3), sol-gel infiltration (4-5), preceramic polymer infiltration and pyrolysis (PIP) (6-8), spray infiltration (9-10), slurry infiltration (11-13), and molten metal infiltration (14-17). While these techniques have been shown to be technically successful, processes such as CVI, PIP, and molten metal infiltration have yet to be proven to be economically viable. The sol-gel process, while more economical than the previously mentioned processes, can only be used to produce oxide based composites. Spray and slurry infiltration are also more economical than these processes. However, work on these processes has concentrated primarily on systems containing large diameter monofilament fibers. While large diameter fibers have been shown to have desirable properties, they are not easily used in the manufacture of complex 3-dimensional shapes. Dow's approach to the CFCC program was to determine if a low cost manufacturing route based on traditional tape casting methods could be used in the manufacture of small diameter fiber containing composites.

Tape casting has been traditionally utilized in the electronics business for the manufacture of multi-layer substrates and packaging (18). In this process, ceramic powders are mixed with polymer binders and plasticizers and then cast into thin sheets or tapes using a die system. These tapes are then stacked and laminated into multi-layer structures. After removal of the binders and plasticizers, the laminates can then be consolidated into dense articles.

The basic concept for tape casting a composite is shown schematically in Figure 3. As shown, traditional tape casting techniques are used to cast matrix materials into 2-D fiber preforms to form monolayer tapes. However, the objective of this work was to obtain a homogeneously distributed matrix material throughout a fiber preform. The implication of the process shown

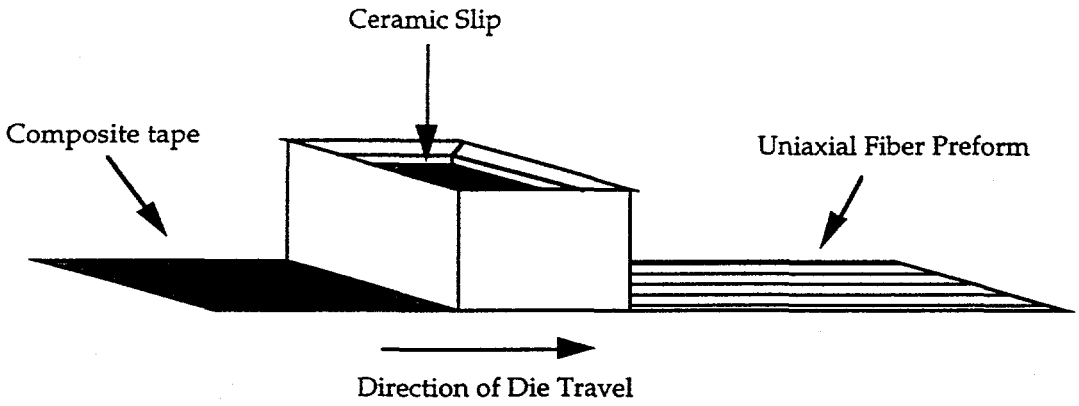

Figure 3. Schematic representation of tape casting technique for infiltrating fiber preforms.

in Figure 3 is that the fiber infiltration process during casting is critical to obtaining a high quality composite.

Previous work on tape casting of composites has avoided this issue by casting the matrix material as a monolithic sheet and then alternating layers of these sheets with layers of fibers during the lamination process (eg. 19-23). However, this process has only been used with larger diameter monofilament fibers where material flow during densification is sufficient to provide a uniform composite. For multifilament fiber tows, this process cannot provide the necessary uniformity to obtain high performance composites. Since the objective of this work is to develop processes capable of making shaped articles, multifilament fibers are a requirement. Commercially available monofilament fibers are large diameter (>50μm) and are consequently too stiff to allow fabrication of complex shapes.

While there are numerous factors which influence the quality of monolithic tapes (e.g. particle size distribution, dispersion, viscosity, rate of solvent removal, shrinkage, etc...), using the tape casting process to manufacture composite materials brings additional factors into play. For instance, in traditional tape casting, fairly high viscosity formulations (~ 10,000 cps) are used to improve tape quality. Use of lower viscosity levels often leads to cracking in the monolayer tapes which can lead to other difficulties during subsequent processing steps. However, formulations prepared at the higher

viscosity levels cannot homogeneously infiltrate a multifilament fiber preform. Consequently, optimization of viscosity is key to making a good composite.

In addition, obtaining high green strength and flexibility in as-cast tapes is different for monolithic and composite tapes. Because of the structure imparted to the tape by the fiber preform, flexibility in a composite tape is much more difficult to obtain through chemical means than it is in a monolithic tape. As has previously been mentioned, flexibility is a requirement in the manufacture of shaped components. Dow's approach to resolving this issue was to examine both chemical and physical modifications to the traditional tape casting process. From the chemical side, we have worked with a variety of commonly used binder/plasticizer systems to develop a system that would optimize the tape qualities necessary to obtain a high performance composite. From the physical side, we have developed new die systems and casting procedures to help improve the infiltration process.

B. Experimental Procedure

For this program, one of Dow's patented self-reinforced silicon nitrides (SRSN) was chosen as the matrix material (24). Studies to determine appropriate casting compositions were based on the matrix composition shown in Table II. All components shown were attrited, dried and sieved to a 60 mesh to provide a uniform powder for formulating tape casting slips. All slip systems were prepared with soluble polymer binders and plasticizers. Slip systems were chosen based on traditional polyvinyl butyral and polyacrylate binder systems. Hydroxypropyl methylcellulose (METHOCEL* E15-LV Premium) was also explored as a water based binder system. In all cases, pre-solubilized binders were used in conjunction with powdered binders to provide the appropriate binder/plasticizer ratio and

*Trademark of The Dow Chemical Company

Component	Volume %
Si_3N_4	94.50
Y_2O_3	2.90
MgO	1.60
SiO_2	0.82
Ta_2O_5	0.17

Table II. SRSN composition used in Phase I.

polymer/solvent contents. Homogeneous binder/plasticizer/ceramic systems were prepared by roll mixing for 8 hours. Zirconia milling media was used to reduce undesirable contamination during the mixing process.

Screening of slip systems was conducted by evaluation of cast monolithic (no fibers) tapes. For this screening, casting was done on MYLAR™ film coated glass plates. Slips were filtered through 70μm nylon mesh screens prior to casting. For each system, tapes were cast at a 0.76 mm thickness. Solvent removal was done under non-flowing conditions within a solvent hood.

For modification and/or optimization of a slip system, composite tapes were evaluated. In this case, fiber preforms were prepared by uniaxially aligning Ceramic Grade NICALON™ fiber tows on the tape casting plate. Lay-up was done either by hand, or using an automated fiber prepregger with the resin bath removed. Infiltration of the preforms was done using a variety of modified tape casting dies, as will be described in later sections. Casting thickness and solvent removal rates were similar to those used in making monolithic tapes.

Prior to this cooperative agreement, several surface active agents were identified as providing good dispersion of the SRSN system. However, in high polymer content tape casting systems, competition for active sites on powder surfaces may occur. Consequently, additional work was required to optimize systems containing both surfactants and polymer binders and plasticizers. For this work, dispersion quality was determined from viscosity

measurements. Slips were prepared using the methods described above. Viscosity was measured on a computer controlled Brookfield viscometer under ambient temperature conditions.

Mechanical analysis of modified formulations was done by testing 1.27 cm x 2.54 cm monolayer tapes in 3 point bending with a span of 1.9 cm. Loading rate was kept constant at 0.5 mm/minute. All specimens were unloaded after a fixed displacement of 3.8 mm. As there is a difference in surface quality between the top and bottom of cast tapes, all monolayers were tested with the bottom surface in tension.

C. Results and Discussion

1. Tape Systems

The standard polyacrylate system is shown in Table III. For this system, toluene is used as the solvent, Acryloid B-82 and A-10S are used as binders and PX-316 and Paraplex PG-60 are plasticizers. To explore the effects of increasing the binder and/or plasticizer content on tape quality, slips were made with the compositions shown in Table IV. During the drying process, all of the tapes made cracked severely. Based on the cracking observed, it was determined that either the shrinkage in this system was too high and that a higher solids loading would be necessary, or that the solvent evaporation rate was too high.

Because of the fine grain size of the SRSN material, high solid containing slips are difficult to obtain without flocculation and subsequent increases in viscosity. Consequently, high solid content slips were prepared with a surfactant to improve the dispersion and keep the viscosity at a manageable level. The composition of the slips prepared is shown in Table V. In this case, the solids content for each of the slips has been increased compared to the original slips. Binder and plasticizer contents have been varied to examine their effect on tape quality. As with the previously prepared tapes, tapes prepared with these formulations also showed severe cracking during the drying process.

Component	Volume %
SRSN	30.64
Toluene	51.54
Acryloid B-82	6.90
A-10S	1.76
PX-316	5.07
PG-60	4.09

Table III. Composition of Acryloid based slip system for tape casting

	Volume %			
Component\Slip	1	2	3	4
SRSN	31.69	29.97	31.45	29.64
Solvent	52.24	50.41	52.34	51.10
Total Binder	8.90	8.58	6.65	10.50
Total Plasticizer	7.17	11.04	9.56	8.77

Table IV. Binder and plasticizer content for various tape formulations evaluated in Phase I.

	Volume %						
Component\Slip	1	2	3	4	5	6	7
SRSN	35.28	35.52	36.37	35.05	41.87	40.75	38.11
Solvent	50.11	50.44	51.66	49.78	48.51	47.22	47.01
Total Binder	7.82	4.92	8.06	10.68	4.17	5.64	11.61
Total Plasticizer	4.54	6.86	1.60	2.26	2.78	3.80	0.85
Surfactant	2.24	2.26	2.31	2.23	2.66	2.59	2.42

Table V. Binder and plasticizer content for high solids tape formulations evaluated in Phase I.

The solvent removal process for these tapes consists of simple evaporation under non-flowing conditions. Consequently, a chemical modification of the solvent system must be made to reduce the evaporation rate. The evaporation rate of organic liquids can be related to the vapor pressure and subsequently to the boiling point of the liquid. An increase in the boiling point of the liquid would imply a decrease in the evaporation rate, all other conditions remaining the same. An effective means of changing the boiling point of solvents is through the use of a mixture of solvents. In addition, there are potential benefits to the use of a zeotropic mixture of two solvents. 2,6, dimethylpyridine will form a zeotropic mixture with toluene and raise the boiling point from 110°C to 144°C. However, this mixture has potential health hazards associated with it and was consequently ruled out as a potential system for exploration. Several azeotropic mixtures can be formed with toluene, but all effectively have reduced boiling points compared to toluene. Because of these problems, and the fact that polyacrylates are known to be fairly unforgiving binder systems, further work on this system was not conducted. Instead, the majority of the remaining work was done using the polyvinyl butyral (PVB) system.

The standard polyvinyl butyral system is shown in Table VI. For this system, a 60/40 mixture of ethanol and o-xylene (by weight) has been used for the solvent system. Butvar 98 and 73 are polyvinyl butyral binders, and UCON 50-HB-2000 and PX-316 are used as plasticizers.

2. Tape Formulation Viscosity

Unlike the polyacrylate system, this formulation can be used to make crack-free monolithic tapes. However, as formulated in Table VI, this slip is too viscous to be useful in infiltration of fibrous preforms. For this reason, a series of experiments was conducted to examine the effect of commercially available surfactants on the viscosity of the polyvinyl butyral casting system. The surfactant which showed the most improvement was a

polyvinylpyrolidone based surfactant known as Ganex® P-904 (GAF Chemical).

Component	Volume %
SRSN	29.2
o-xylene	29.5
Ethanol	27.8
Butvar 98	1.9
Butvar 73	4.7
PX-316	4.9
UCON 50-HB-2000	2.0

Table VI. Composition of polyvinyl butyral based slip system for tape casting

Figure 4 shows the viscosity of the polyvinyl butyral system as a function of Ganex® P-904 content. As can be seen, the viscosity of these slips at any level of surfactant shows some shear rate dependence. However, in traditional tape casting processes, high shear rates are not seen. Consequently, a comparison of the effect of surfactant level can be limited to the lower shear rates on the graph in Figure 4. Results show that the viscosity can be dropped from a level of 8000 cps for a slip with no surfactant to a level of 3500 cps for a slip with 2.25% surfactant (surfactant levels are based on the weight of the ceramic powder only). Castings prepared with this formulation showed improvement in matrix infiltration into fiber tows. However, while infiltration of the matrix into individual fiber tows was improved through the use of the reduced viscosity slips, the overall composite still lacked the high flexibility and strength needed for downstream processing into small diameter tubular shapes.

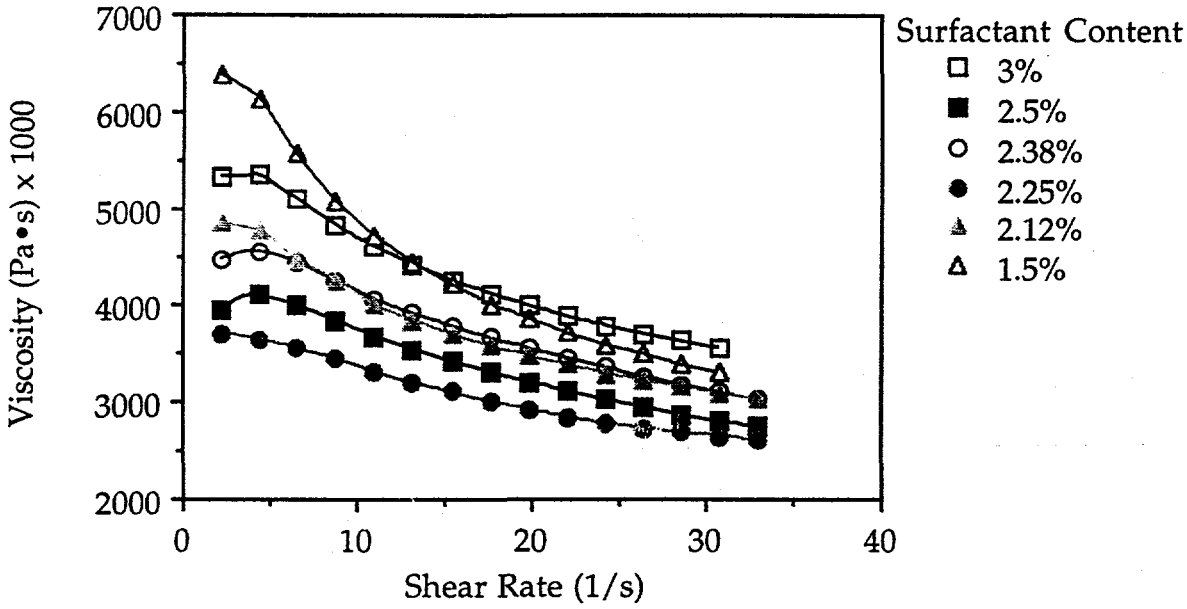

Figure 4. Viscosity as a function of shear rate and surfactant content.

3. Tape Flexibility

To better understand the strength and flexibility of these composites, a series of formulations was made with varying binder/plasticizer ratios. During this work, formulations were developed which have lead to improved flexibility. However, strength was found to be more a function of the physical nature of the casting rather than the chemistry of the formulation. Modifications to the tape casting die system were used to address the strength and will be discussed in a later section.

Table VII shows the formulation which was found to have the most improved flexibility compared to the standard formulation of Table VI. To quantify the flexibility of composites made with these formulations, monolayer tapes were prepared using the tape casting process described earlier. Small sections of these tapes were then tested in 3-point bending. Figure 5 shows the flexural behavior of tapes made with the formulations shown in Table VI and VII. The curve labeled "Current Formulation" is for a composite made with the optimized formulation shown in Table VII. As

shown, the current formulation has a much higher yield point, indicating a higher degree of flexibility without inducing permanent damage in the tape.

Component	Volume %
SRSN	29.8
o-xylene	27.7
Ethanol	25.5
Butvar 98	1.4
Butvar 73	3.9
PX-316	6.9
UCON 50-HB-2000	2.6
Ganex P-904	2.2

Table VII. Composition of optimized polyvinyl butyral based slip system for tape casting

In the early stages of this program, it was thought that dry monolayer composite tapes could be wrapped around solid mandrels to form multi-layer tubular components. Consequently, improved flexibility without inducing permanent damage was of critical importance to the component development effort. The impact of this improved flexibility can be directly related to the manufacture of the target components. As previously mentioned, the target components for this program are tubes having a diameter of 10-20 cm. A simple analysis of the bending data generated shows that tapes made from the formulation shown in Table VI cannot be used to make tubes having a diameter less than 1.32 meters without inducing damage into the tapes during the wrapping process. The same analysis shows that tapes made from the improved formulation of Table VII can be used to make tubes of 40 cm and greater. Unfortunately, while this represents a 3-fold improvement in the flexibility, it is not sufficient to provide tubes in the 10-20 cm range. As will be discussed in the component manufacturing section, this problem can be overcome by optimization of the solvent content in tapes during the component manufacturing steps.

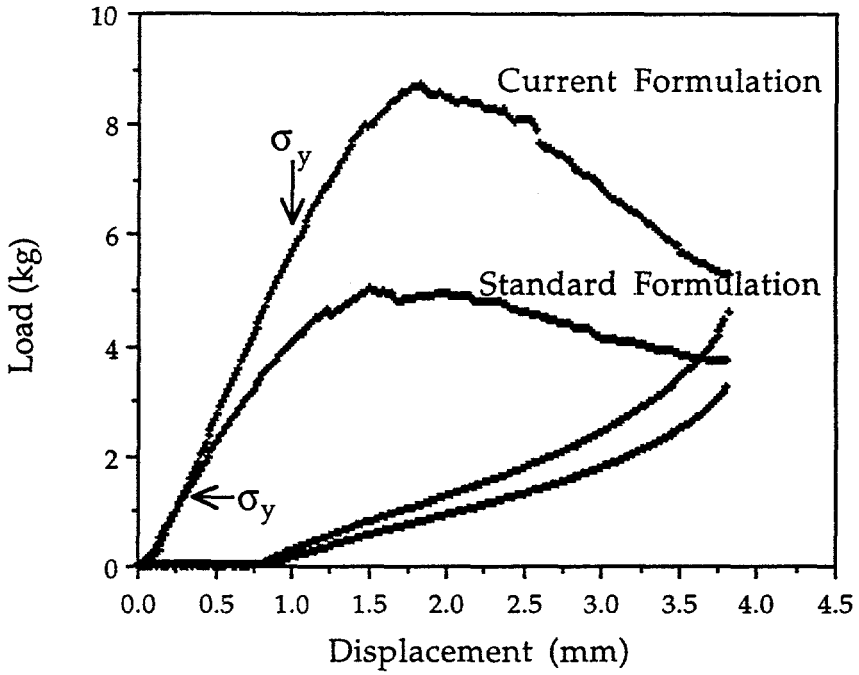

Figure 5. Flexural behavior of standard (pre-CFCC) tape formulation and current tape formulation.

4. Tape Strength

As mentioned previously, chemical modification to formulations can help improve flexibility and reduce slip viscosity to aid in the infiltration process, but additional physical modifications to the casting equipment was also necessary to provide tapes having good handling characteristics. Traditional tape casting dies consist of a main chamber with at least one doctor blade whose purpose is to regulate the thickness of the tape being cast. However, in the manufacture of a fiber composite, additional components are necessary to aid in the infiltration and distribution of the matrix slip into the fiber preform. Figure 6 shows a diagram of a modified die designed at Dow to improve the quality of composite tapes.

During the development of this die design, it was found that using a lower solids content slip to pre-infiltrate the fiber preform helped in the infiltration

process. By itself, this lower solids content slip would not provide the desired matrix content in the composite. However, when used to pre-wet the fiber preform, the infiltration of the primary slip was found to be greatly improved and provided the requisite matrix content. The die design shown in Figure 6 utilizes multiple chambers to allow for the application of this pre-infiltration slip.

This design also utilizes a series of brushes which are located in both chambers. The brushes, which can be used in a variety of positions along the length of the chamber, can be adjusted to regulate the amount of slip which remains in the composite after casting. In addition, these brushes were found to help spread fiber tows and subsequently help in the infiltration process.

Figure 7 shows two uniaxially aligned, monolayer composite tapes prepared by the tape casting method. The tape on the left was made using a standard tape formulation developed prior to Phase I and a traditional tape casting die. The tape on the right was made using the tape formulation changes discussed above and the modified tape casting die. The improvements seen here have provided improved handling and flexibility during the lamination and component fabrication steps. Results from this modified process have also indicated that more consistent infiltration into fiber tows is possible. Figure 8 shows a cross sectional view of a NICALON fiber composite prepared with this process. The distribution of matrix into the fibers tows is homogeneous, as desired.

The combination of the improved die design, the use of a pre-wetting slip, and the improved formulation slips allow the tape casting process to be used to make uniform, high quality composites from multifilament fiber tows. However, while this work was critical for the development of uniform composite microstructures, it is not sufficient to provide the shaped components required for many applications. In the next section, Dow's efforts to use the techniques described above to make tubular components will be discussed.

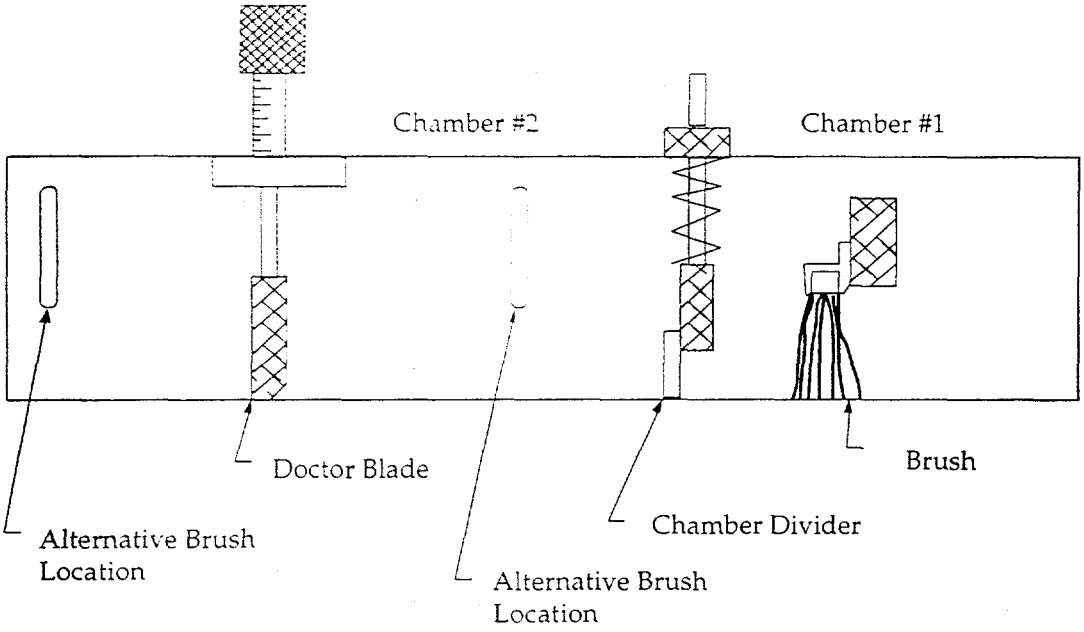

Figure 6. Schematic diagram of tape casting die for infiltration of multifilament fiber tows.

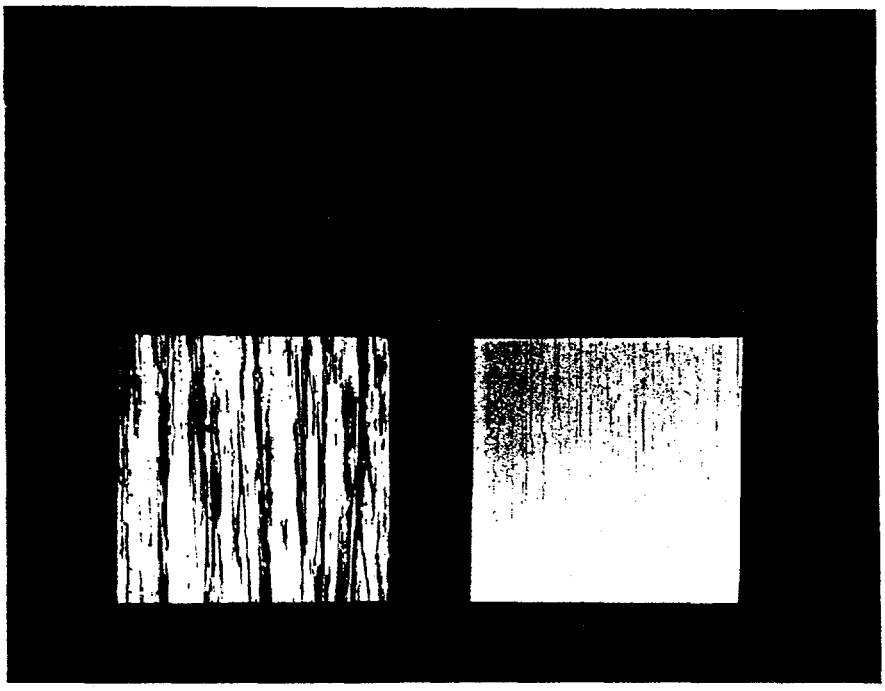

Figure 7. Monolayer tapes prepared by the tape casting technique prior to this cooperative agreement (left) and currently (right).

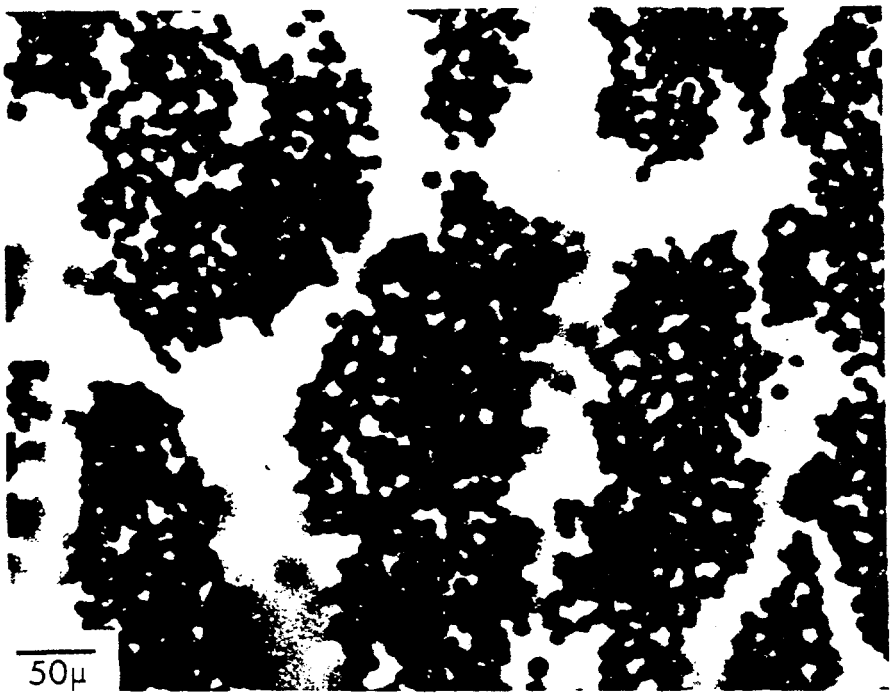

Figure 8. Cross sectional view of composite tape prepared with the tape casting method.

5. Binder Removal

Removal of polymer species (binder, plasticizer & surfactant) from tapes made with the polyvinyl butyral system shown in Table VII cannot be done using a single process environment. As seen in Figure 9, an exotherm occurs during the heating of this system in air. Rapid gaseous evolution from the specimen is thought to occur concurrently with this exotherm. In many cases, this causes the part to break apart during the binder removal process. While the binder can be removed in an inert environment such as nitrogen or argon, these environments leave carbon levels which are unacceptable (see Table VIII). It is well known that the densification of silicon nitride materials is significantly affected by the presence of excess carbon. For this reason, silicon nitride tapes made with the polyvinyl butyral system need to undergo a two step burn out. In the first step, burn out proceeds under an inert environment. Once the temperature reaches the point at which carbon begins to oxidize, oxygen is slowly bled into the system. Table VIII compares

the carbon and oxygen ranges from nitrogen burn out cycles and from the cycle described above.

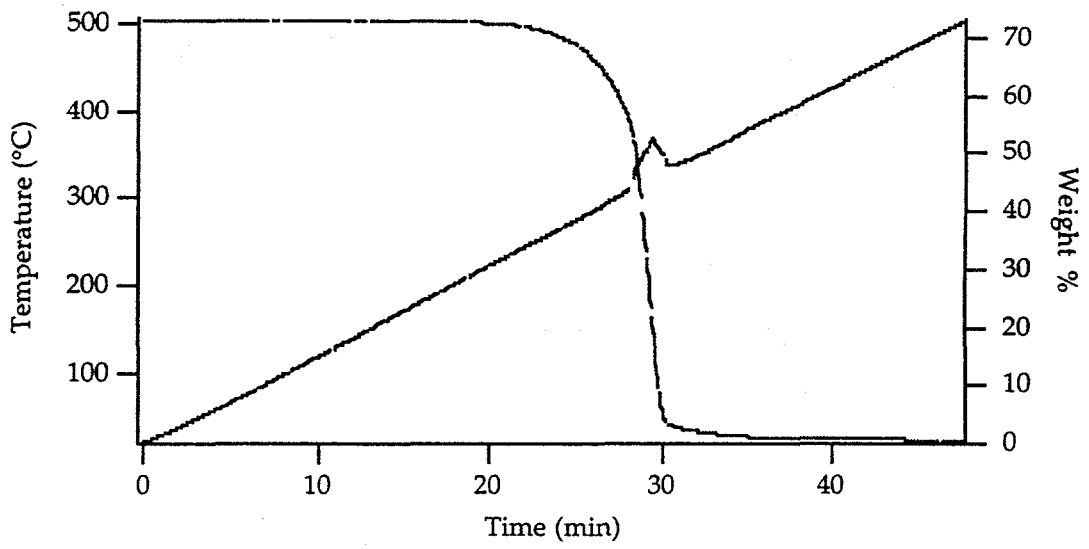

Figure 9. Thermogravametric curve for a SRSN tape made with the polyvinyl butyral system.

Burnout Environment	% Carbon	% Oxygen
Nitrogen	0.3-0.5	3.2-3.4
Nitrogen/Oxygen	0.15-0.18	3.2-3.4
SRSN prior to Burn-out	0.15	3.2

Table VIII. Oxygen and carbon levels after burn out in: A) nitrogen, and B) a combined nitrogen/oxygen cycle.

IV. COMPONENT MANUFACTURE

A. Introduction

As mentioned previously, Dow's target components are cracking tubes for the production of ethylene. These tubes range in size from 10-20 cm in diameter and 4.5-18 meters in length, depending on individual plant design. Ideally, the simplest way to make such a tube is through a filament winding process. While Dow has developed such techniques outside of this program, the objective of this work was to determine if tape casting could be utilized as a more economical means of fabrication.

In order to make a tube from the tape casting process, individual monolayer tapes must be laminated together in tubular form. One possible way to do this is to wrap each monolayer around a core mandrel which can be subsequently removed. However, there are numerous difficulties in reducing this concept to practice. Dow has attempted several techniques for making components and has found one technique, based on controlled solvent content, that provides the high quality necessary for the application. The techniques which were explored, as well as their benefits and drawbacks, will be discussed in the sections to follow.

B. Experimental Procedure

All casting to make composite tapes was done according to the procedures described in the section on Process Development, except were noted. Composites made for the component development effort were made with ceramic grade NICALON fiber and used the slip formulation described in Table VI. For demonstration purposes, the fiber angle in the tubes was kept constant at ±45°. Drying of tapes was done under ambient conditions.

Lamination was done using an isostatic laminator at 70°C and 13.8 MPa. In this unit, pressure is applied via a water bath. Consequently, specimens were double bagged in polyester barrier film bags to protect them from the water during lamination. Pressure was typically applied for 5 minutes.

C. Results and Discussion

Most of the work which was conducted early in the program concentrated on making flat plates which could be used for material property evaluation. Consequently, composite tapes were dried thoroughly, cut to shape, stacked in a uniaxial manner, and laminated using a heated metal die. Obviously, this technique needed modification if tubular shapes were to be made.

Initial attempts at making tubular shapes used fully dried composite tapes that were wrapped around solid aluminum mandrels. However, at the time, the formulation development for cast tapes was not optimized and handling was extremely difficult. Tapes would typically crack along the fiber axis or would buckle perpendicular to this axis because of their lack of strength and flexibility (see Figure 10). The buckling could sometimes be avoided by making larger diameter tubes. However, additional buckling was also seen during the lamination process.

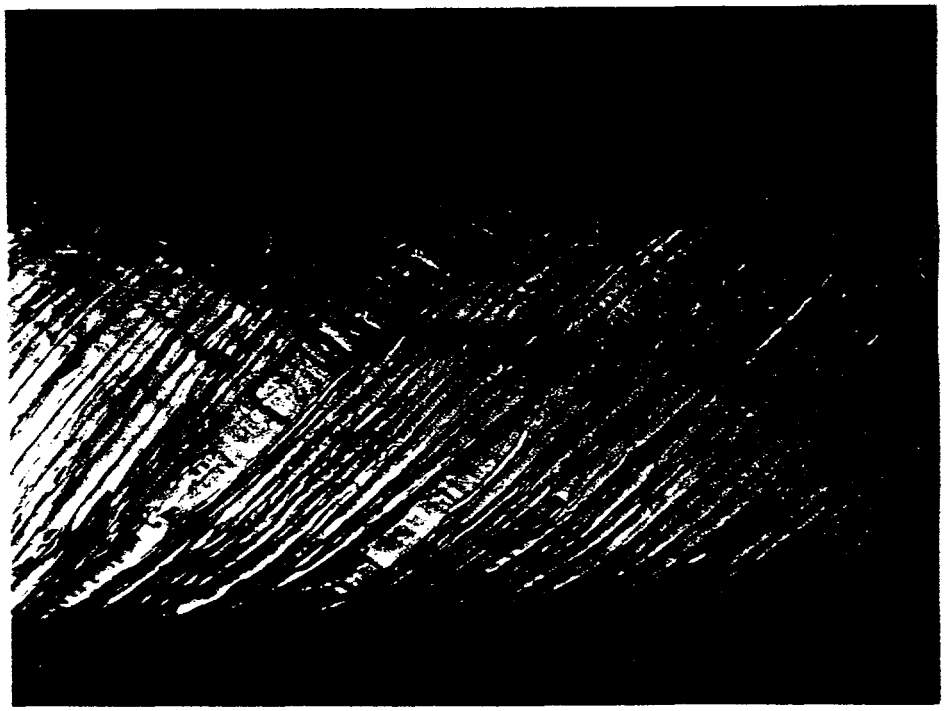

Figure 10. Green CFCC tube showing buckling of fibers.

Lamination of a sufficient number of layers to produce the desired wall thickness cannot be done with a single procedure. Individual composite layers cannot be dry wrapped on mandrels tight enough to avoid major buckling during the lamination process. Consequently, layers were added one at a time, with a lamination step after each layer was added. Clearly, making a usable tube with this technique is extremely labor intensive. However, it is possible to make tubes in this manner under controlled conditions.

This process became significantly easier after the formulation development that was discussed in the previous section was complete. With the composite tapes having improved strength and flexibility, the wrapping process became considerably easier. Unfortunately, the process could still not be used to readily make the small diameter tubes that the application required. Also, as the tube length increased, obtaining high quality tubes became increasingly more difficult.

While working with materials that are continually evaporating solvents is difficult in a manufacturing setting, it was decided to explore this method to determine if small diameter tubes could be made. Figure 11 shows the weight loss from a composite tape as a function of drying time. In the early stages of drying, it was found that the handling of the composite tapes was difficult due to the lack of adhesion between fiber tows. In addition, during the wrapping process, matrix slip was often squeezed out of the fiber tows. This left the tows with insufficient matrix, but also left large matrix rich regions on the surfaces of the layers. After long drying times, the wrapping behavior was similar to when tapes were allowed to dry completely.

It is only in a small, critical region that conditions exist that allow composite tapes to be wrapped around small diameter mandrels successfully. This region is marked in Figure 11. Tubes made with tapes in this region of the drying curve have sufficient flexibility to allow wrapping, while at the same time are dry enough have good inter-tow strength. In addition, the tape is dry enough to avoid the matrix squeezing effect seen with wet tapes. Figure 12 shows a 5 cm diameter 30 cm long tube made by this process.

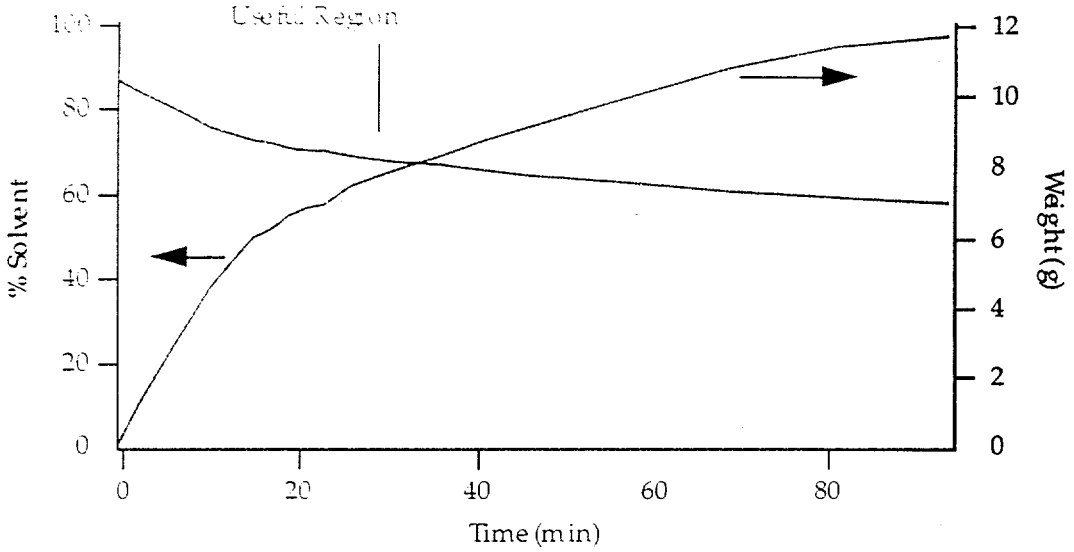

Figure 11. Weight loss as a function of time for a cast tape.

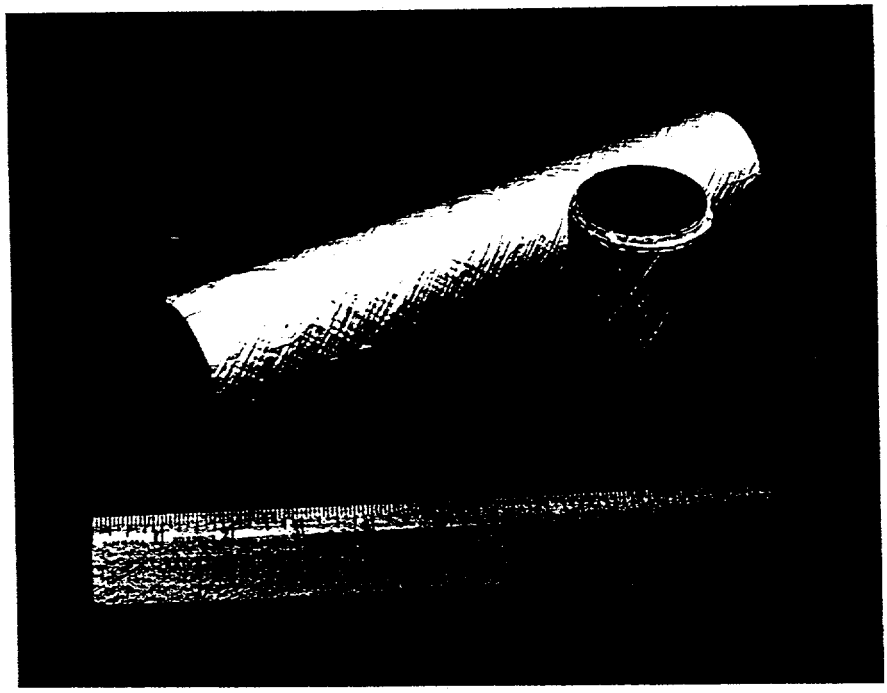

Figure 12. Green composite tube made via the tape casting process.

While this tube is 30 cm long, longer tubes could be made. Dow's tube length was limited by the dimensions of the lamination press. The press available for use in this program had a maximum length of 33 cm. However, larger capacity presses are readily available on the market. In addition, while the fiber angle was kept at ± 45° for most of the tubes made, this technique allows for fiber angles ranging from 0° to 90° at this tube diameter and larger.

V. DENSIFICATION

A. Introduction

While the ability to manufacture long green tubes is important, another factor which is equally important is the densification of these tubes. Because the end use will require that the tubes be gas tight and chemically corrosion resistant, there cannot be an open pore network in the tubes. Consequently, the final density must be near theoretical density. Unfortunately, the densification of most ceramic materials is dramatically altered by the presence of a fully dense second phase, since the second phase does not undergo mass transport to the extent that the primary phase does.

One possible way around this is to process the composite starting with a green ceramic fiber. In this way, the fiber would also shrink during the densification process and help relieve stresses that would otherwise cause cracking or porosity. There are several problems with this approach though. First, it requires a sinterable fiber that does not significantly outgas (as would a polymer derived fiber). While possible to make (25), this type of fiber is not yet commercially available. The second problem with this is that it would require the in-situ development of an interfacial coating that would provide the weak interface needed for fiber pullout. While the commercially available dense fibers have other difficulties, for these reasons outlined above, the current work was limited to using fibers that were fully converted and dense prior to processing.

It is well known that many commercially available ceramic fibers degrade at the temperatures which are typically used to densify monolithic non-oxide ceramic materials (26-30). For this reason, many composite manufacturers have moved to costly and time consuming techniques such as chemical vapor infiltration (CVI) or pre-ceramic polymer infiltration and pyrolysis (PIP). However, full density using these techniques has yet to be realized. Some reaction based processes exist which can obtain full density at moderate temperatures. However, these typically leave residual metals which can be detrimental to elevated temperature mechanical properties and the chemical resistance of the composite. For these reasons, this program has examined modifications to more traditional ceramic processing methods, despite the fiber degradation issues.

Polymer derived ceramic fibers degrade at elevated temperatures by two mechanisms: grain growth and evolution of gaseous reaction species (26-30). While grain growth will degrade the overall properties, gas evolution can both degrade the final properties and inhibit the densification process. Silicon dioxide and free carbon present in the fibers can react to form gaseous SiO and CO which can bloat specimens during densification. The temperature at which this occurs is environment dependent. Obviously, since this program is utilizing conventional powder processing techniques, elevated temperatures (>1400°C) will be required to process these composites. Consequently, an understanding of the temperature limits of the fibers is critical to obtaining fully dense articles.

In addition to fiber degradation issues, the densification of most ceramics can be enhanced by the application of external pressure. Some studies have also shown that pressure can reduce the fiber degradation seen in polymer derived fibers (28-30). Consequently, part of this study examined the effects of pressure on densification of CFCC's made from the tape casting process.

B. Experimental Procedure

Fiber degradation studies were conducted in high temperature graphite furnaces. Fiber specimens were placed in graphite crucibles with lids. In all

cases, heat up rates, hold times, and gas flow rates were kept at levels similar to that used to densify the matrix material. The fibers examined were 1) Ceramic Grade NICALON fiber, 2) TYRANNO™ fiber, and 3) HPZ™ fiber. Evolution of CO as a function of temperature was determined via a CO monitor with a collection port near the crucible lid.

Densification experiments were conducted in two stages. In the first stage, flat plate composites were prepared via the tape casting process. In the second stage, tubular composites prepared via the methods described above were examined. Experiments were done as a function of temperature and pressure. Experiments under flowing gas conditions were conducted in Astro™ high temperature graphite furnaces. Intermediate pressure levels were obtained in a graphite lined over-pressure furnace. Specimens were placed in either graphite or BN crucibles. In some cases, specimens were packed in a powder bed. The powder bed used had the same composition as the matrix SRSN.

High pressure levels were obtained using an ASEA hot isostatic press. Closed systems were obtained by encapsulating specimens in glass. In these cases, encapsulation was done in-situ during the densification run. Temperatures were increased under vacuum to the softening point of the glass, at which point a minimal pressure was applied to provide a seal for the glass capsule. Several encapsulation techniques were used and will be described in the following section.

C. Results and Discussion

1. Fiber Degradation

Figure 13 shows CO evolution as a function of temperature for NICALON fibers, TYRANNO fibers, and an SRSN/NICALON fiber composite under the conditions in which Dow typically densifies it's SRSN materials. Also shown in this figure is a baseline CO curve for the matrix without fibers present. Here, CO is presumed to evolve from the small amounts of free carbon present in the matrix as well as from the carbon in the furnace itself.

For the TYRANNO fibers, evolution of CO begins to occur at a temperature of 1425°C. The NICALON fibers begin to show this gas evolution at a slightly higher temperature of 1650°C. This difference is expected since TYRANNO fibers have a higher SiO_2 and free carbon content than NICALON fibers. The results for the SRSN/NICALON fiber composite show that the temperature at which CO begins to evolve is shifted to much lower temperatures (ca. 1250°C) and maintains a low evolution rate up to about 1600°C. This is most likely due to reaction of the carbon and SiO_2 with the oxide species present in the matrix material. These results on fiber degradation lead to the conclusion that major CO evolution can be avoided during densification of SRSN/NICALON fiber composites at temperatures below 1600°C. Above this temperature, fiber degradation will be significant and composite properties can be expected to drop off accordingly. In addition, holes in the fibers and matrix can be formed as gas is evolved from the fibers. These holes can lead to greatly exaggerated grain growth in the matrix (Figure 14) as well as significantly reduce the strength of the fibers.

While the NICALON fibers and TYRANNO fibers have significant amounts of both SiO_2 and free carbon which cause fiber degradation, fibers such as HPZ silicon nitride fibers have considerably less of these species and are reported to retain their strengths above 1300°C (31). Consequently, their use could potentially raise the upper densification temperature limit by approximately 100°C over NICALON fiber composites. Figure 15 shows the CO evolution from the NICALON fibers, TYRANNO fibers, HPZ fibers and for an empty crucible. These results show that the CO evolution from the HPZ fibers is on the same order of magnitude as the empty crucible. Because of this, these fibers would be expected to maintain their properties to higher temperatures than either NICALON fibers or TYRANNO fibers. HIGH-NICALON fiber, a low oxygen grade of SiC fiber, would be expected to yield similar results to the HPZ fiber. However, the main drawback to the use of either HPZ or HIGH-NICALON fibers is their prohibitively high cost.

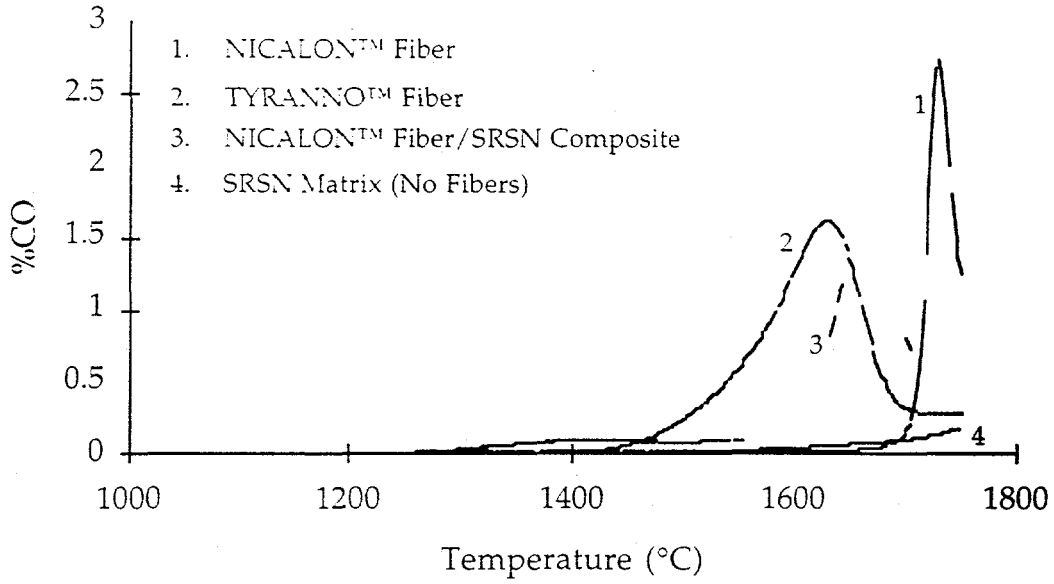

Figure 13. Carbon monoxide evolution as a function of temperature.

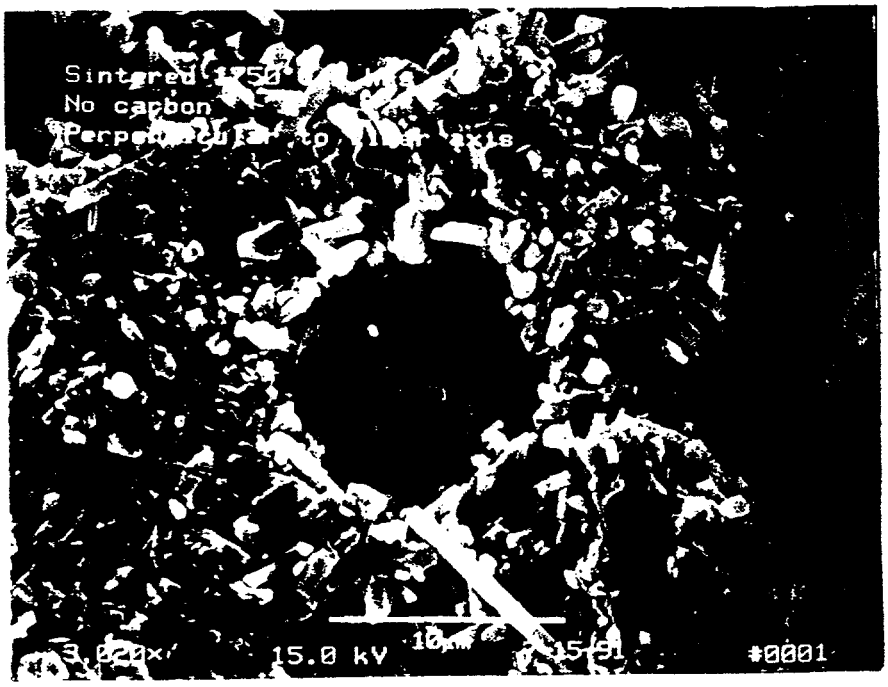

Figure 14. Micrograph of NICALON fiber/SRSN specimen sintered at 1750°C for 3 hours.

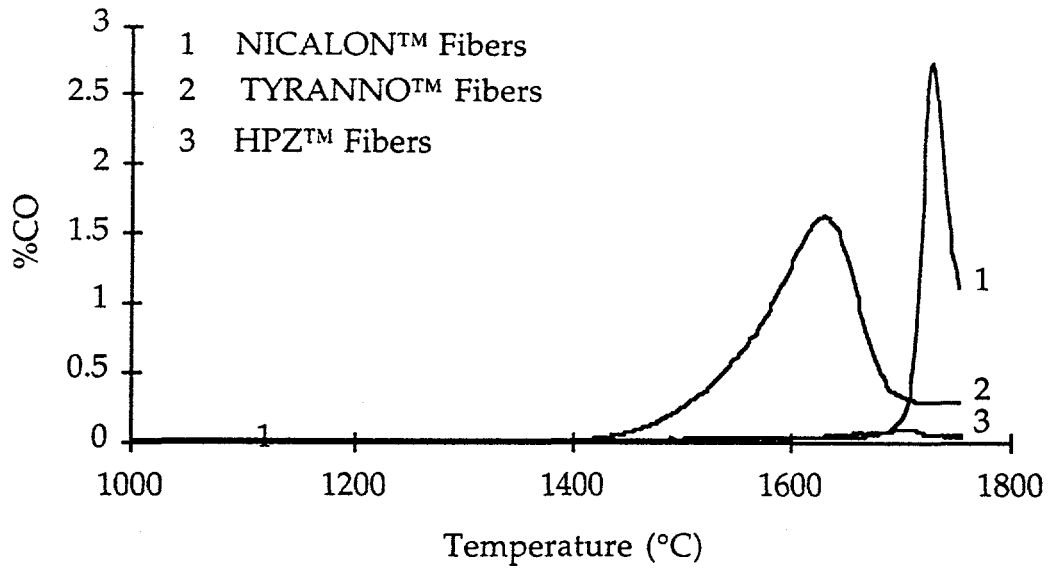

Figure 15. CO evolution from NICALON, TYRANNO, and HPZ fibers as a function of temperature.

The economics of manufacturing tubes for this application were discussed in section IIB and were based on a fiber cost of $660 per kilogram of fiber. The current cost of HIGH-NICALON fiber is $13,992/kg. Assuming that volume usage could drive down the cost as low as $2800/kg, the cost per tube would still increase from $203M to $410M (see Table IX). Clearly, this will have a major impact on the cost/performance window. For the application Dow has chosen, the increased cost outweighs the potential performance benefits at these prices.

2. Composite Densification

The implication of these results is that pressureless sintering of SRSN/NICALON fiber composites at or above 1600°C will be significantly hindered by gas evolution. The results shown in Figure 16 are for a temperature of 1600°C and show that fully dense composites can be obtained through the use of high pressures. Typically, our matrix material, self reinforced silicon nitride, is hot pressed at 1825°C. While CFCC's can be made this way, some fiber degradation occurs at this elevated temperature,

	Cost Estimate $/Tube	Capital Cost $/Unit/Yr
Fiber	250,496.83	0
Fiber Coatings	89,463.20	0
All Other Materials	13,276.03	0
Total R.M.	253,236.06	0
Labor, Utilities, Waste Disposal, Maintenance	9,466.47	0
Overhead, Depreciation, DFC,Taxes	5,904.00	35,786.75
R.M. Inventory	0	13,537.62
In-Process Inventory	0	2,629.03
Transfer Inventory	0	5,296.04
Total Bulk	368,606.62	57,249.44
Packaging	1,108.59	0
Total Plant	369,715.21	57,249.44
Selling, Gen. & Adm., Research, Cash & Acc.	40,975.91	76,532.27
Inventory for Sale	0	27,132.19
Total Cost per Tube	410,691.03	160,913.90
	410,691.03	160,913.90

Table IX. Preliminary process economics based on fiber cost of $2800/kg.

and parts are limited to extremely simple shapes. Dow has explored several other means of densifying these type of composites ranging from pressureless sintering to hot isostatic pressing. Appendix C outlines the conditions that were examined in this study.

As shown in Figure 16, >97% theoretical density can be obtained using hot isostatic pressing techniques. However, as with any hot isostatic pressing technique where closed porosity in the specimen has not been obtained, transfer of these high pressures to the specimen can only be obtained by means of an encapsulation process. While this is a fairly straight forward process for flat plates, encapsulation of tubular components is more complex. Obtaining a good seal is critical to pressure transfer. If a hole is present in the capsule, the pressure will equilibrate on the inside and outside and the part will see no pressure. In this case, you are in a similar situation to over pressure sintering, and full density in the part will not be obtained.

However, in addition to obtaining a complete seal around the specimen to obtain adequate pressure transfer, Dow's application requires that parts maintain good concentricity. The concentricity requirement is there for two

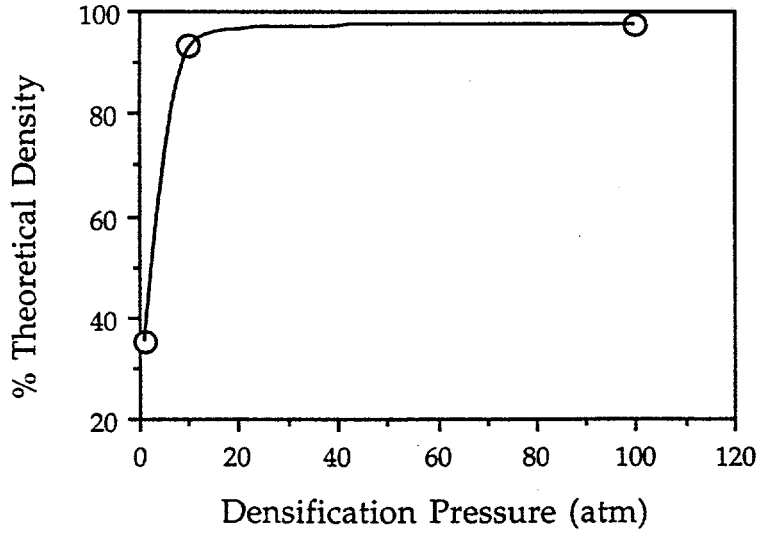

Figure 16. Density of SRSN/NICALON fiber composite as a function of densification pressure at 1600°C.

reasons. First, since the final part for this application is much larger than can practically be manufactured in one piece, smaller tube sections will need to be made and joined together to form the final part. Concentricity of parts insures that each piece will fit with all other pieces during the joining process. Secondly, even if pieces could be joined that were not concentric, the final part would have steps or ridges that would create gas flow problems and lead to increased coke build-up.

Figure 17 shows a small tube that was encapsulated in glass and densified using Hot Isostatic Pressing (HIP'ing). While fully dense, clearly, the tube is not concentric along its length. For this reason, Dow has chosen to explore the use of solid tubular inserts to help maintain concentricity during application of pressure. Figure 18 shows two cross sections of encapsulation designs. Design A has a solid graphite inner core with the tubular specimen on the outside of it. It has the advantage of being fairly easy to assemble, although obtaining a gas impermeable seal is still an issue. Design B has a graphite sleeve on the outside of the part. As will be seen later, this design is better than the one shown on the left.

All pieces made with the internal graphite sleeve showed evidence of cracking, and very few showed evidence that they had sealed properly. Figure 19 shows a piece which reached full density with this technique. This specimen is typical of those tested with this configuration. The recovered piece was broken in numerous places parallel to the tube axis. This type of cracking is indicative of hoop stresses in the tube. This is not surprising considering that the thermal expansion coefficient of graphite is considerably less than that of the composite ($\alpha_{graphite} = 2x10^6$, $\alpha_{composite}=5x10^6$).

By moving to Design B of Figure 18, extreme cracking like that shown above can be avoided. With the part on the inside of the sleeve, the part is free to contract inward upon cooling, thus reducing the thermally induced stresses. Figure 20 shows a small tube manufactured by this process. In this case, while concentricity was maintained, the part did not fully densify due to insufficient sealing. While it is the belief of this researcher that full density parts with good concentricity can be obtained from this technique, no fully

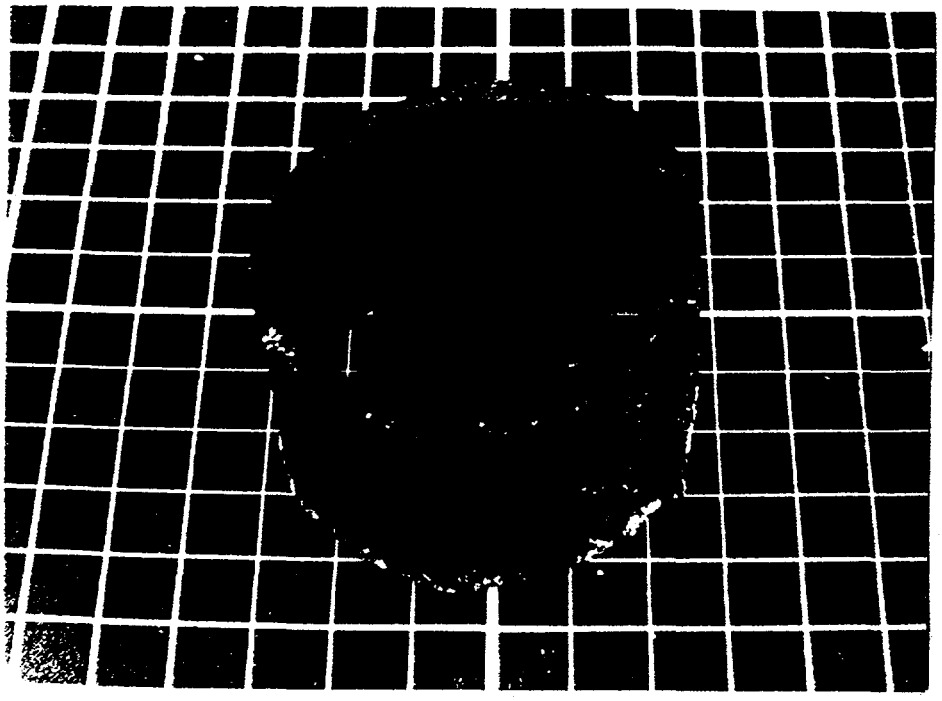

Figure 17. CFCC tube prepared by glass encapsulated HIP'ing with no support structure.

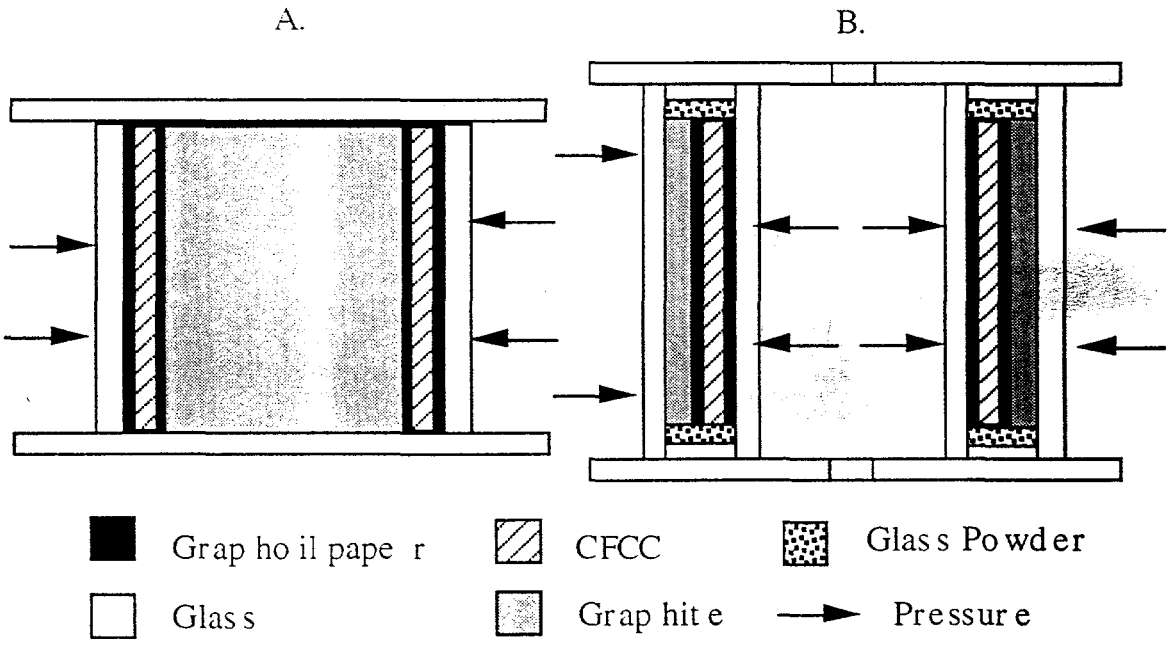

Figure 18. Glass encapsulating designs with A) a solid graphite inner core and B) a solid graphite outer sleeve.

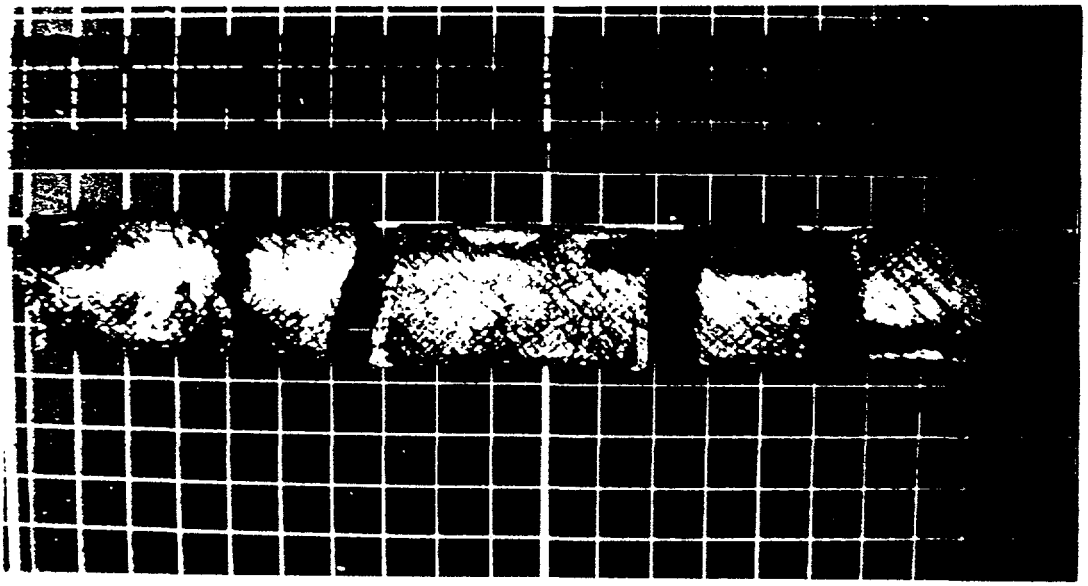

Figure 19. CFCC tube prepared with Design A from Figure 17.

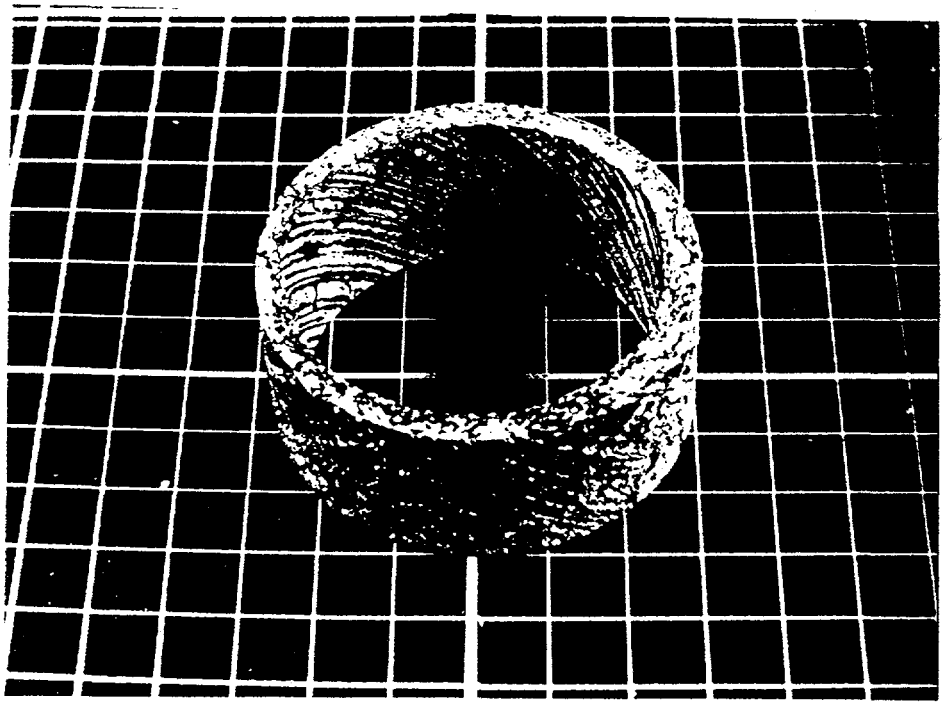

Figure 20. CFCC tube prepared with Design B from Figure 16.

dense tubes were made from this technique as part of this study. In addition, glass encapsulated HIP'ing is one of the least desirable densification processes from a manufacturing perspective.

3. SRSN Matrix Compositions

During the densification tasks of this program, it was found that the composition of the matrix was critical to obtaining good composites. As can be seen in Appendix C, several matrix compositions were explored. The differences are mainly in the composition of the glassy phase and the resulting microstructure. Self reinforced silicon nitride can have a variety of microstructures. However, in all cases, the microstructures are defined by elongated β-Si_3N_4 grains. The elongated grains are typically formed during densification when α-Si_3N_4 grains undergo a solution-precipitation process in the glassy phase. Figure 21 shows a typical SRSN microstructure.

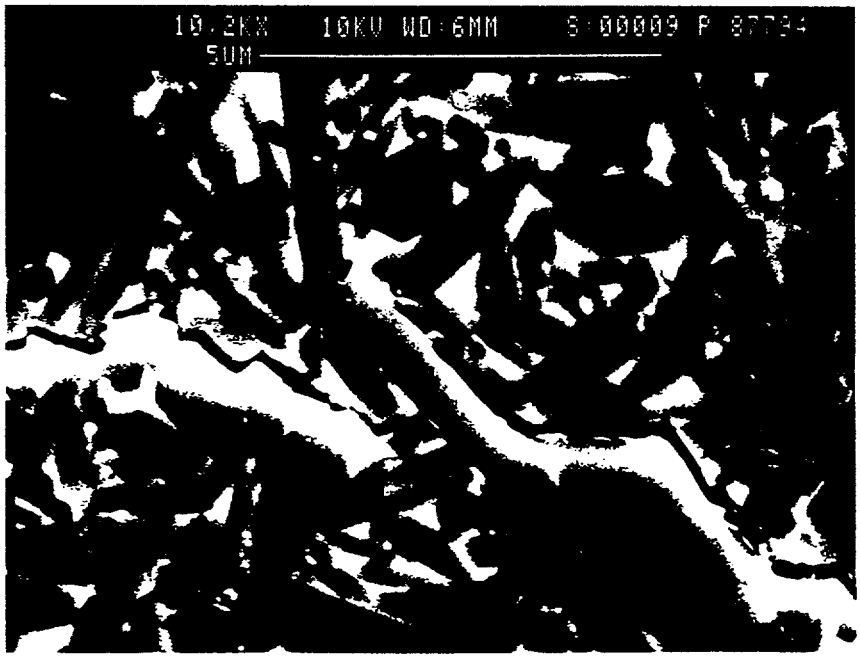

Figure 21. Typical SRSN microstructure.

The chemistry of the system is one factor which influences the extent and aspect ratio of elongated grain formation. In this study, the presence of NICALON fibers has been found to affect the grain development. Composition SN-A was described previously in Table II and the microstructure shown in Figure 21. In comparison to this, a typical microstructure of a NICALON composite prepared with the SN-A composition is shown in Figure 22. As can be seen, the extent of elongated grain development is diminished in the case of the composite. While this will provide a matrix with lower toughness than is desired, the elongated grains which are present have a dramatic effect on the properties.

Figure 23 shows the microstructure of a NICALON composite prepared with Composition SN-B. Work by Lee et. al. (32) has shown that densification is enhanced when using β-Si_3N_4 instead of α-Si_3N_4. The SN-B composition utilizes seed crystals of β-Si_3N_4 to try to enhance the sinterability of the material. The microstructure of a typical monolithic SN-B composition is similar to that shown in Figure 21. However, in the case of the composite, no evidence of elongated grains exists. Analysis of this material reveals that, instead of forming acicular β-Si_3N_4 grains, a mixture of equiaxed SiO_xN_y and β-Si_3N_4 grains forms. Clearly, this material would be expected to behave differently than the material of Figure 22.

Figure 24 shows an acoustical C-Scan image of a NICALON composite made with the SN-B composition. This image reveals a crack that runs perpendicular to the fiber axis. This type of cracking can be seen in a majority of specimens made with the SN-B composition and is indicative of residual stresses in the material. Since the thermal expansion along the fiber axis is less than that of the matrix, tensile residual stresses are expected during cooling from the densification temperature. In this case, the reduced toughness due to the change in microstructure is most likely insufficient to keep flaws from propagating under the residual stress. In addition, a large area of reduced density is also revealed in the middle of this specimen. This variation in density can be attributed to the extent of reaction of the matrix and fibers, which varies from the middle of the specimen out to the edges. Neither the cracking nor the large variation in microstructure are seen in

composites made with the SN-A composition. For this reason, most of the work done in this program is with the SN-A composition.

However, a limited number of experiments were also conducted with Composition SN-C (see Appendix C). This composition was previously developed to allow for a lower densification temperature than the SN-A composition in monolithic components. However, NICALON composites made with this composition were not found to exhibit differences in densification behavior compared to those prepared with the SN-A composition and additional work was not pursued.

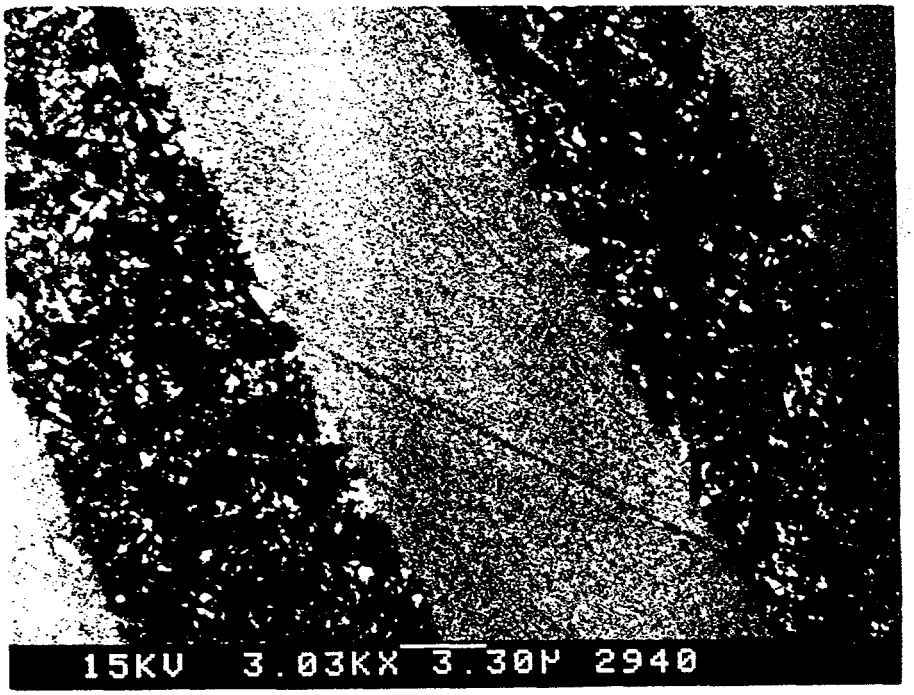

Figure 22. Typical microstructure of NICALON/SRSN composite made with the SN-A Composition.

Figure 23. Typical microstructure of NICALON/SRSN composite made with the SN-B Composition.

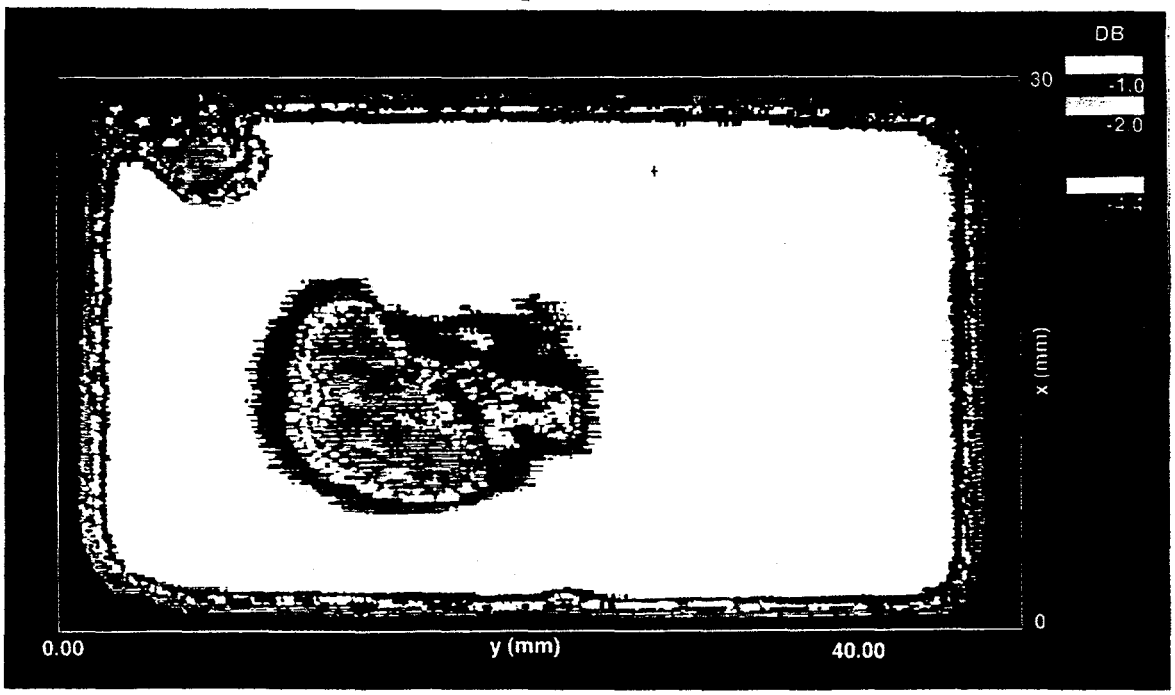

Figure 24. C-scan image of a NICALON fiber/SRSN composite made with the SN-B composition.

Note on NDE:

As CFCC's proceed into the commercialization stages of development, the use of NDE techniques will become critical as quality inspection tools. For Dow's target application, the high up-front cost of the component makes premature failure from processing defects unacceptable. The defects that may need to be detected range from large macroscopic flaws, like those seen in the C-scan image shown in Figure 24, to finer microstructural features such as the fiber alignment seen in the X-ray image shown in Figure 25.

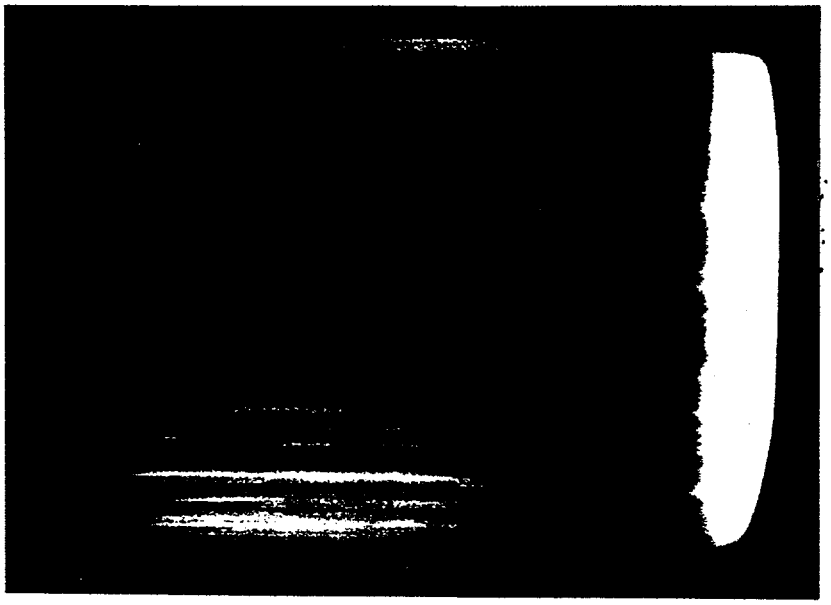

Figure 25. X-ray image of a NICALON fiber/SRSN composite made with the SN-A composition.

4. Process Environment

In addition to chemistry effects, the densification of silicon nitride is also affected by the process environment (33). For this reason, sintering experiments were conducted in both graphite crucibles and in BN crucibles. In the case of the graphite crucibles, specimens were packed in a powder bed of similar composition to the matrix itself. It is well known in the industry that sintering of silicon nitride in graphite crucibles can be enhanced through the use of powder beds. However, as the results of Appendix C show, no measurable difference in density between specimens prepared in graphite crucibles and BN crucibles was found for either the SN-A or the SN-B compositions.

VI. INTERFACIAL MODIFICATION

A. Introduction

As with any ceramic fiber composite, the composite properties of Dow's CFCC's are strongly dependent on both the fiber properties and the fiber/matrix interfacial characteristics. Not surprisingly, composites made with un-coated fibers have varying properties which depend on the extent of fiber/matrix reaction, but in general show extremely poor properties. For Dow's CFCC program, numerous fiber/fiber coating systems were screened for potential improvements in composite properties. The fibers examined were NICALON fibers, TYRANNO fibers, and NEXTEL™ 550 fibers. Limited evaluation of HPZ fibers was also conducted. The fiber coatings examined were primarily in the family of ceramic carbides and nitrides: TiC, TiN, TiB_2, ZrN, ZrC, and C.

In addition to the chemical composition at the interface, the properties of the composite are also affected by the thickness of the coating, the extent of coverage of the coating, and the extent of fiber degradation during the coating process. Also, the stability of the interface under operating conditions is a critical parameter in the development of useful CFCC's for long life applications.

B. Experimental Procedure

Fiber coatings for this task were applied by both 3M and General Atomics, the majority being done by 3M. In both cases, chemical vapor deposition (CVD) was used to apply the coatings. Coatings applied by 3M were requested to have a carbon interlayer of 500Å and a primary coating thickness of 800Å. The primary coatings requested were described in the introductory section above. Coatings requested from General Atomics were to have primary coating thicknesses of 0.2, 0.3, and 0.5 μm, and in the case of ZrC, a carbon interlayer of 500Å. The primary coatings requested were TiN, ZrN, and ZrC.

Composites were prepared with coated fiber using the tape casting procedures and formulations described in section III.C. Fibers were aligned in a uniaxial direction prior to casting. No surface treatments were done on the as-received coated fiber prior to casting. All composites were hot pressed at 1825°C under 34.47 MPa pressure for one hour. Billets were then machined into 3 x 4 x 45 mm chevron notch specimens for toughness testing using the process defined in ASTM STP 855. Testing was done on an Instron 8562 testing machine. Loading was applied under three point configuration at a loading rate of 1μm/min.

C. Results and Discussion

1. Un-coated Fibers

As mentioned in the introductory section, the properties of composites made with un-coated fibers is generally poor. The reason for this is both a strong fiber/matrix bond and fiber degradation. Figure 26 shows the fracture surface of a hot pressed NICALON fiber/SRSN composite where the fibers were processed without an interfacial coating. Clearly, no evidence of fiber pullout has occurred and the flaw has propagated directly through the fibers. This type of behavior is indicative of a strong fiber/matrix bond. In addition, the grain size has increased considerably in the fibers. Increases in grain size have been shown to have disastrous effects on the strength of the fibers.

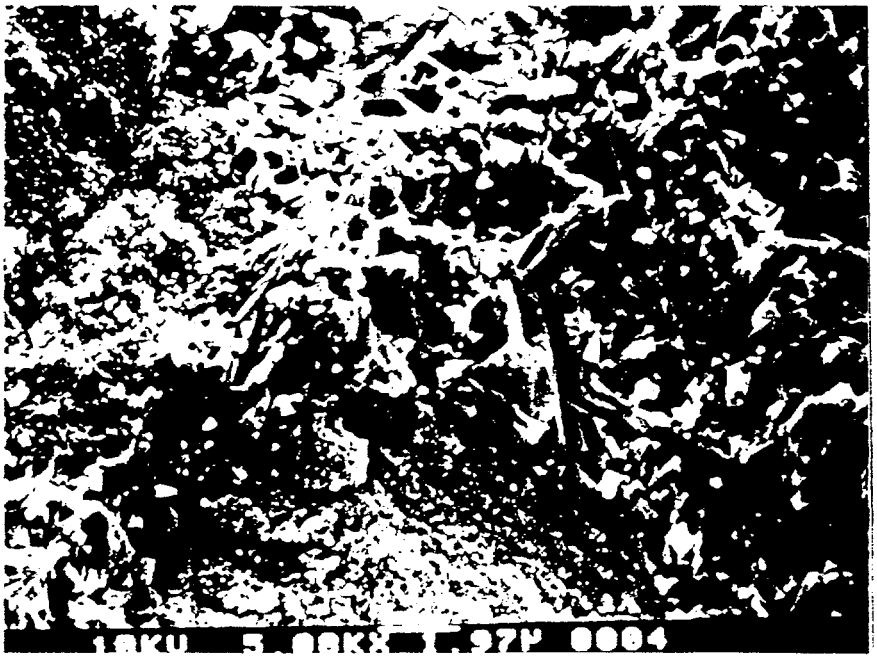

Figure 26. Fracture surface of a hot pressed NICALON fiber/SRSN composite with no interfacial coating.

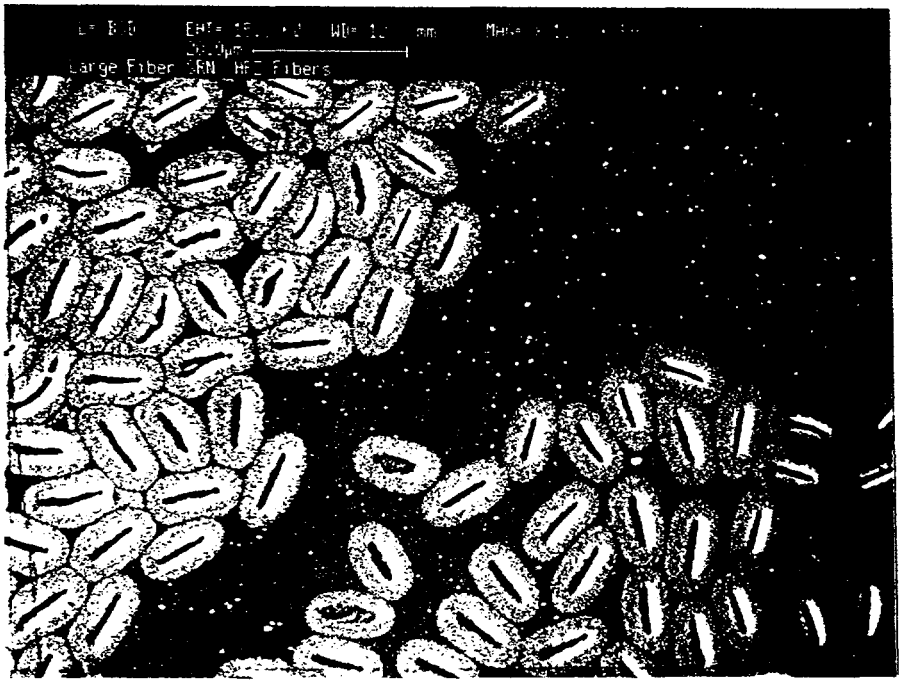

Figure 27. Polished cross section of an HPZ fiber/SRSN composite with no interfacial coating.

Reactions with the fibers can also affect the strength of fibers under certain conditions. Figure 27 shows a micrograph of an SRSN composite prepared with un-coated HPZ fibers. In this case, the fibers have reacted to leave voids at the centers of the fibers. The reaction mechanisms for this system are not yet understood. However, this type of reaction is clearly deleterious to the properties of the overall composite.

2. CVD Coated Fibers

One of the simplest coatings which can be applied is carbon. In addition to being easy to apply, thin coatings of carbon have also been shown to be useful in providing fiber pullout in some systems (34-35). However, carbon is often difficult to keep from reacting during composite processing. Carbon coated NICALON fibers were received directly from Dow Corning and processed into an SRSN matrix as part of this project. However, at the elevated temperatures needed for densification, the carbon simply reacted with the oxide species present in the glassy phase of the matrix. Consequently, a strong fiber/matrix bond was established and fracture occurred in a similar manner to that shown in Figure 26.

For many of the composites made with coated fiber, no evidence of fiber pullout was observed and measured mechanical properties were poorer than for a monolithic SRSN. In the case of the composites made with NEXTEL 550 fiber, none of the composites made showed improved properties. The results of the Chevron notch testing are shown in Figure 28-30. For this material, it was hoped that the interfacial coatings would provide some protection from reaction of the oxide fibers with the glassy phase in the silicon nitride. However, after densification, no definable interface could be found. Testing results clearly indicate a strong fiber/matrix bond in these systems.

Results of composites made with coated TYRANNO and NICALON fibers were considerably more promising. For these materials, the properties measured were a function of both the type of fiber and the fiber coating. In the following discussion, the results will be divided into fiber coating type.

Figures 31 and 32 show the results of the Chevron notch testing of the specimens made with TiC coated TYRANNO and NICALON fibers, respectively. In both cases, the properties of the overall composite has been degraded in comparison to a monolithic SRSN. Fracture surfaces look similar to that of Figure 26 and indicate that strong fiber/matrix bonding is present.

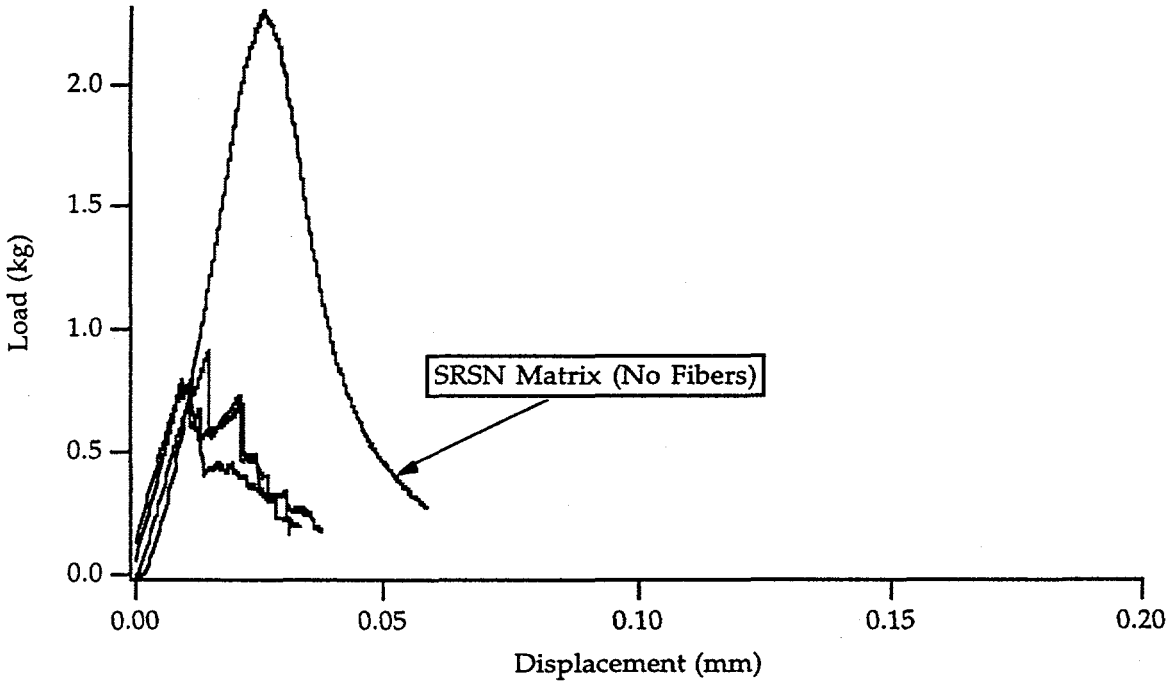

Figure 28. Load-Displacement curve for SRSN composite made with TiB_2 coated NEXTEL 550 fiber.

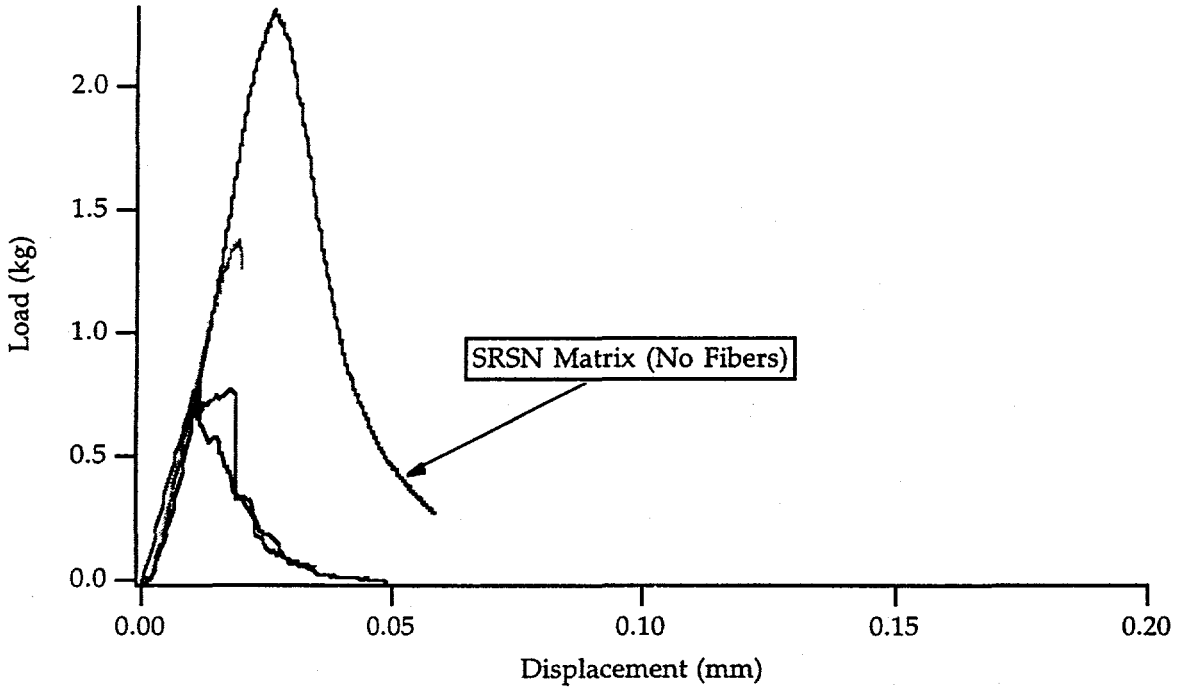

Figure 29. Load-Displacement curve for SRSN composite made with TiN coated NEXTEL 550 fiber.

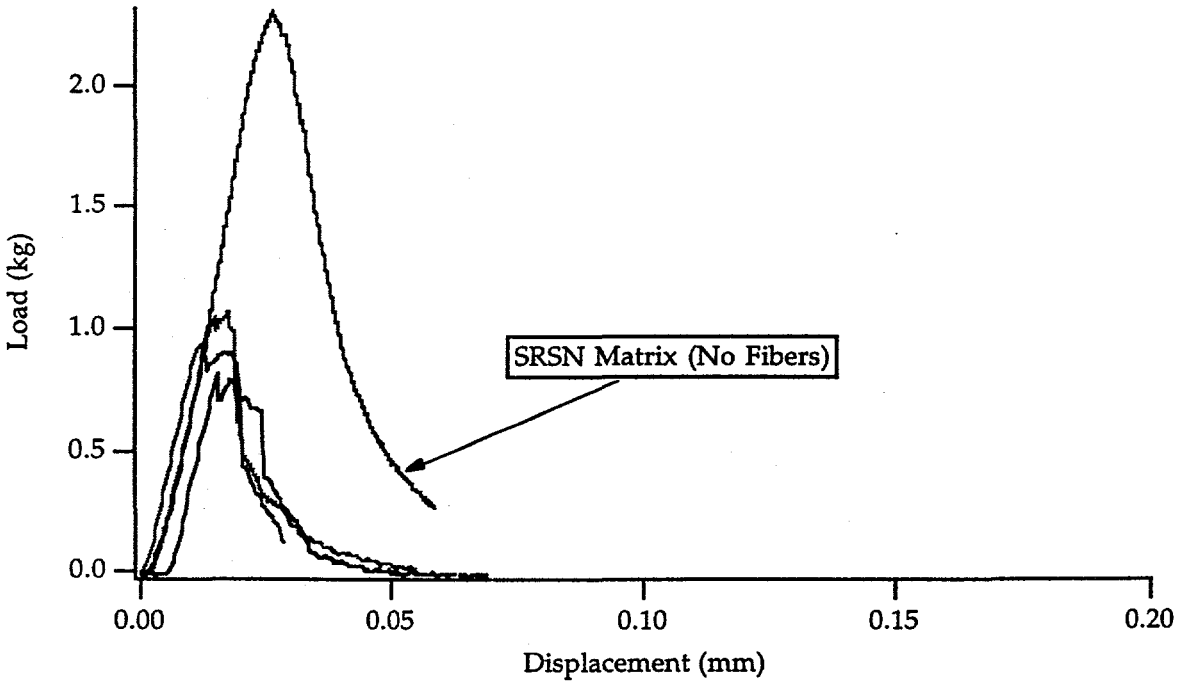

Figure 30. Load-Displacement curve for SRSN composite made with ZrC coated NEXTEL 550 fiber.

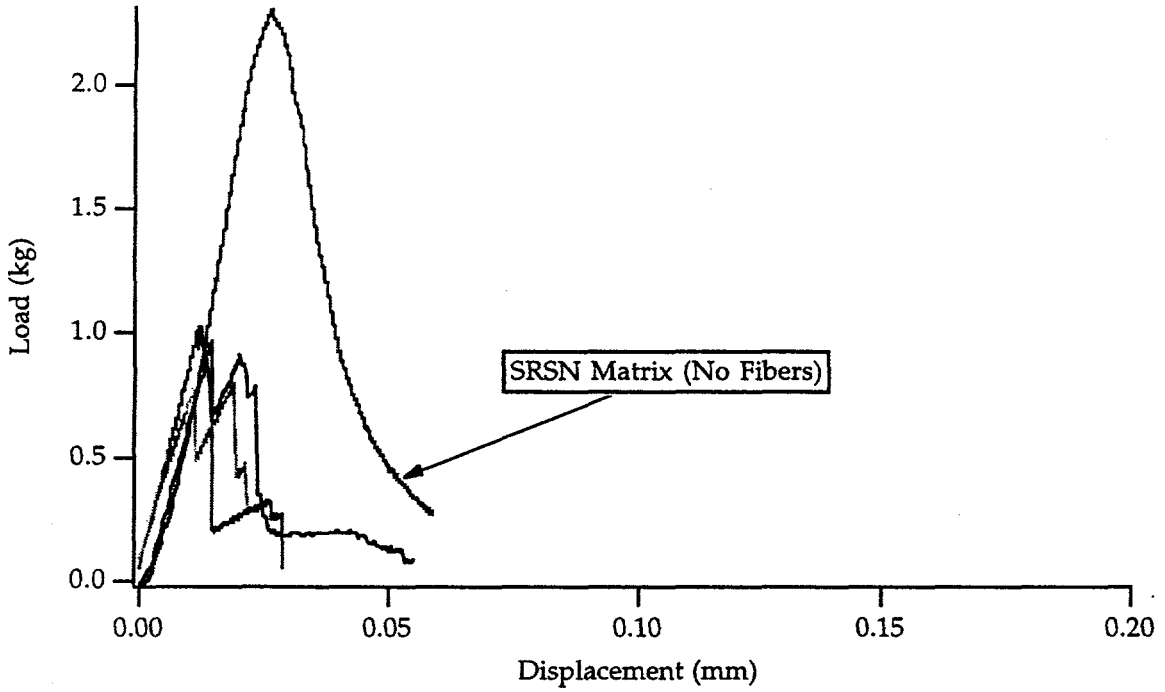

Figure 31. Load-Displacement curve for SRSN composite made with TiC coated TYRANNO fiber.

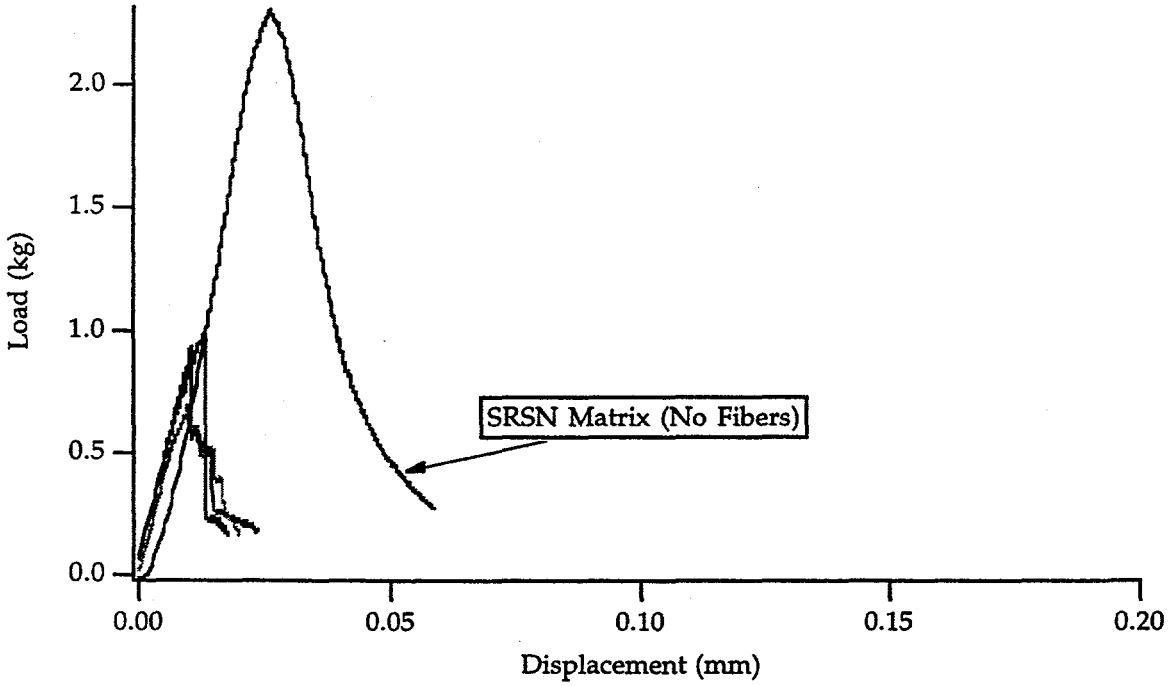

Figure 32. Load-Displacement curve for SRSN composite made with TiC coated NICALON fiber.

Results for the TiN coated fibers were better. Figure 33 shows that, for the TiN coated TYRANNO fibers, the peak loads achieved for these materials were slightly lower than for the matrix alone. However, the frequent rise and fall of the load after the peak is indicative that some toughening in this system is occurring. Figure 34 shows the results for the TiN coated NICALON fiber. Like the previous case, this material also shows signs that limited toughening has occurred. In this case, however, the peak loads are comparable to the matrix alone.

Figure 35 shows a fracture surface of a composite made with TiN coated NICALON fiber. As can be seen, fibers have been pulled out from the matrix. Pullout lengths are only on the order of 10μm. It is this limited pullout that has lead to the behavior seen in Figures 33 & 34.

To understand this behavior, the mechanisms of fiber pullout must be understood. Most theories on fiber pullout relate the pullout length to the

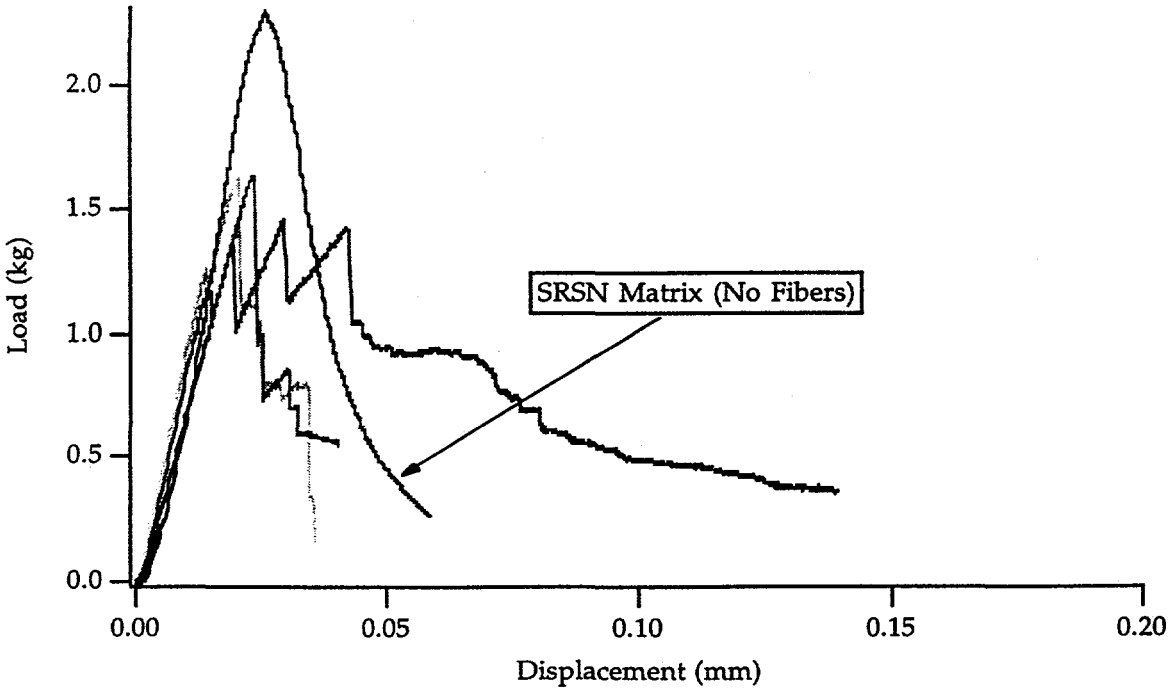

Figure 33. Load-Displacement curve for SRSN composite made with TiN coated TYRANNO fiber.

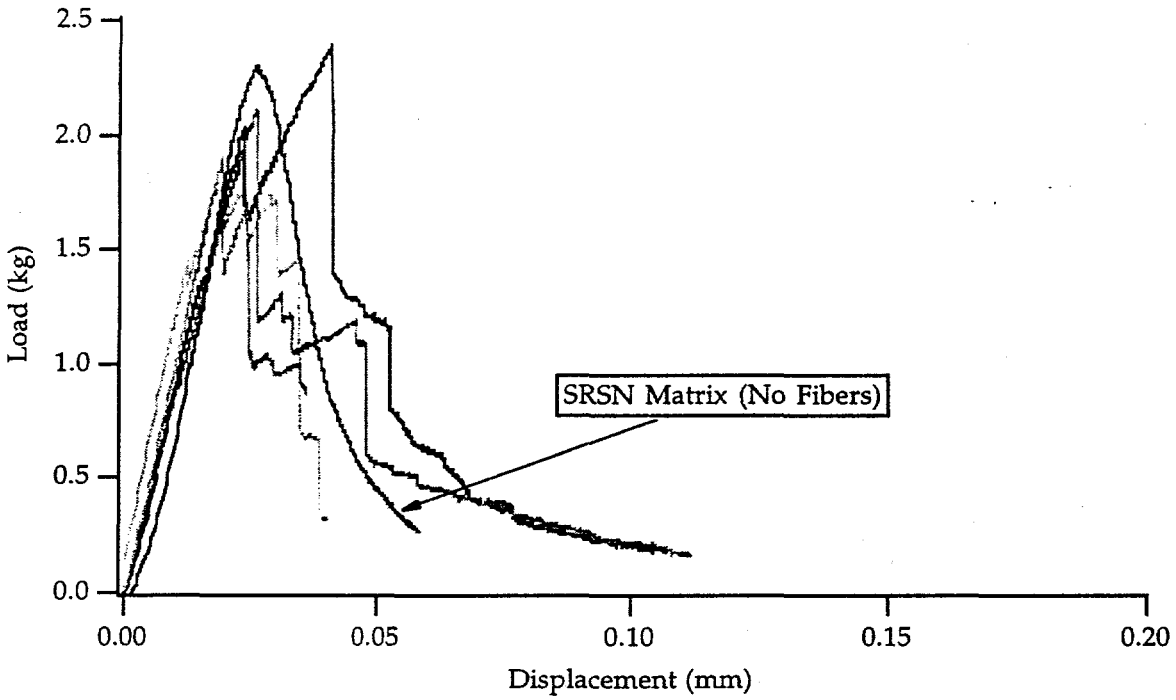

Figure 34. Load-Displacement curve for SRSN composite made with TiN coated NICALON fiber.

interfacial shear strength and to the fiber strength (e.g. 36-37). As can be seen in Figure 35, grain growth in the NICALON fiber has occurred during the densification process. Since fiber strength reductions can be directly linked to grain growth in these systems, fiber pullout lengths will clearly be limited. In addition, it is thought that fiber/matrix bonding in this system is quite high. Figure 36 shows a scanning electron microscope (SEM) photograph of the as-received TiN coated NICALON fiber. The bright area at the edge of the fibers is the TiN coating. Transmission electron microscopy of fibers has shown that for both the NICALON and TYRANNO fibers, coating thicknesses averaged 300Å, but covered only about 60% of the surface of the fibers. After composite densification, the coating had clearly left the fiber surface open to reaction with the fibers (see Figure 37). Given this fact, it is surprising that any fiber pullout has occurred in this system. However, it does indicate that with optimized coatings this system may have potential for improved properties.

The system which has shown the most potential, however, is the ZrC system. Figures 38 and 39 show the results of Chevron notch testing for composites made with ZrC coated TYRANNO and NICALON fibers, respectively. Results from the TYRANNO fiber composites are similar to what was seen in the case of TiN coated TYRANNO fibers. The only difference being that the peak loads are slightly higher. However, results from the ZrC coated NICALON fiber composites show dramatic improvements. As can be seen in Figure 39, peak loads for these composites exceed that of the matrix alone, and fiber displacements are considerable larger (note the change in scale in Figure 39 compared to previous graphs).

The variation seen in the results shown in Figure 39 are most likely due to processing variations. Because of the cost of coated fiber used for this screening, limited amounts of each fiber coating were available. Each coated fiber was found to exhibit different handling characteristics, and composite quality varied considerably during the green processing steps. This variation is easily translated to the variations seen in final properties. However, as

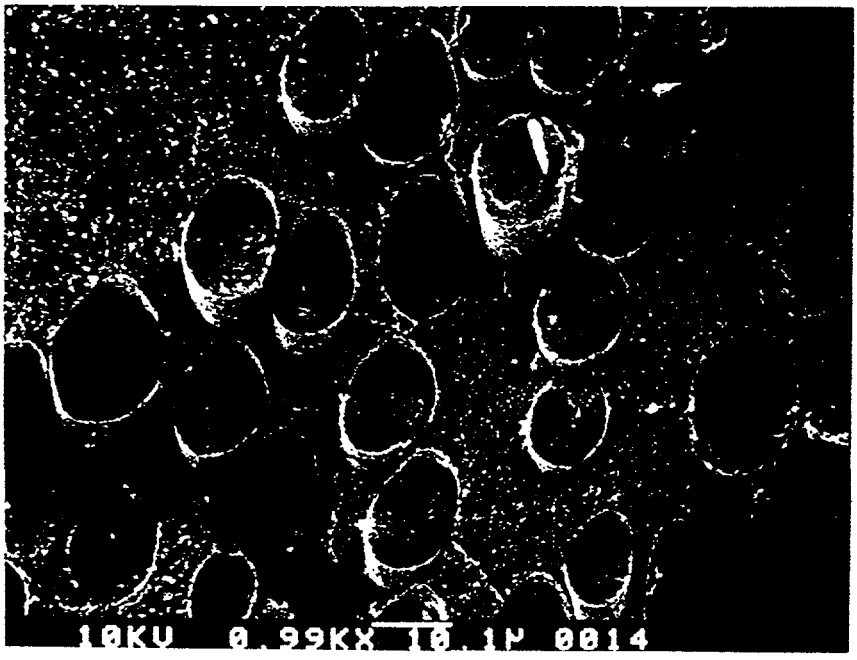

Figure 35. Fracture surface of composite made with TiN coated NICALON fibers.

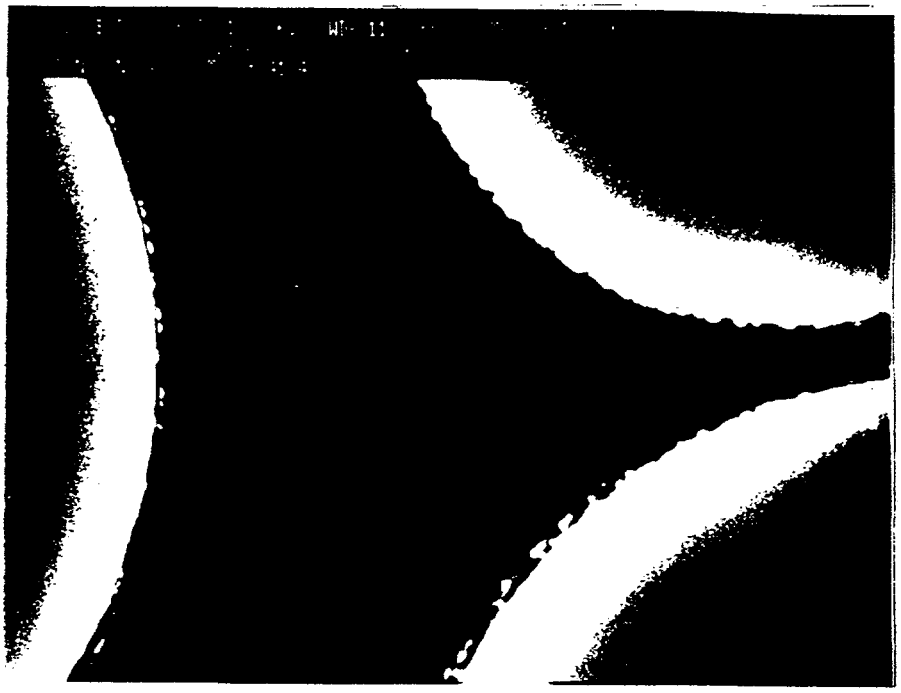

Figure 36. Scanning electron micrograph of as-received TiN coated NICALON fibers.

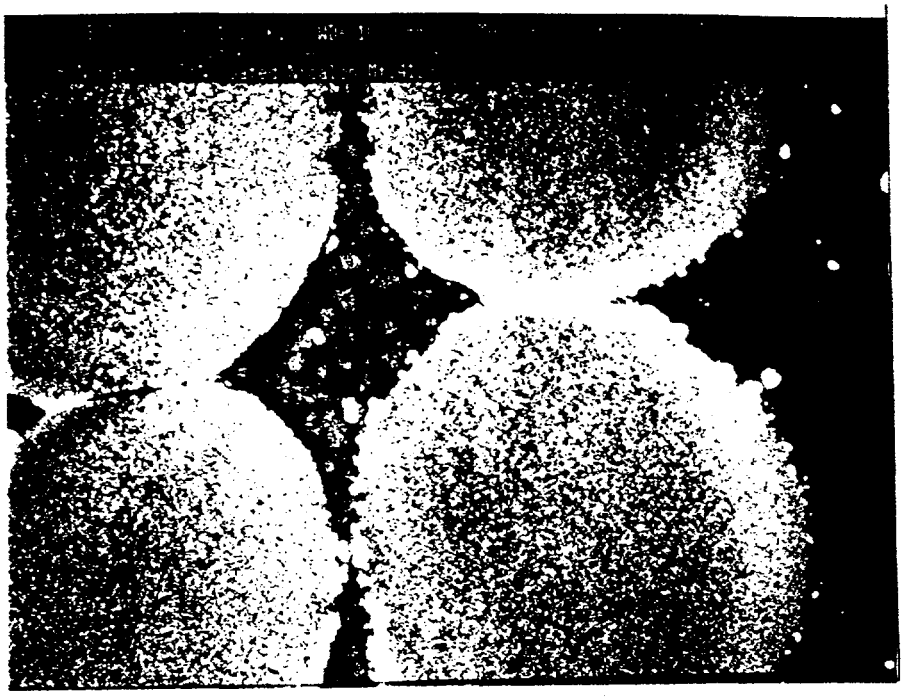

Figure 37. Polished cross section of densified composite prepared with TiN coated NICALON fibers.

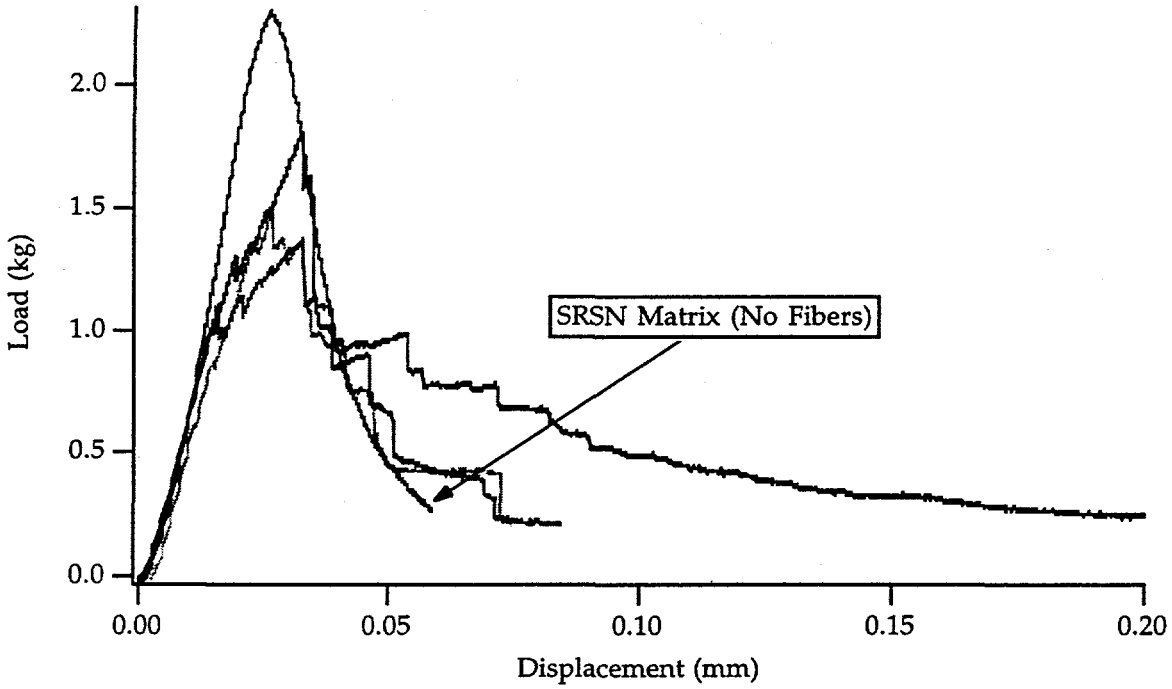

Figure 38. Load-Displacement curve for SRSN composite made with ZrC coated TYRANNO fiber.

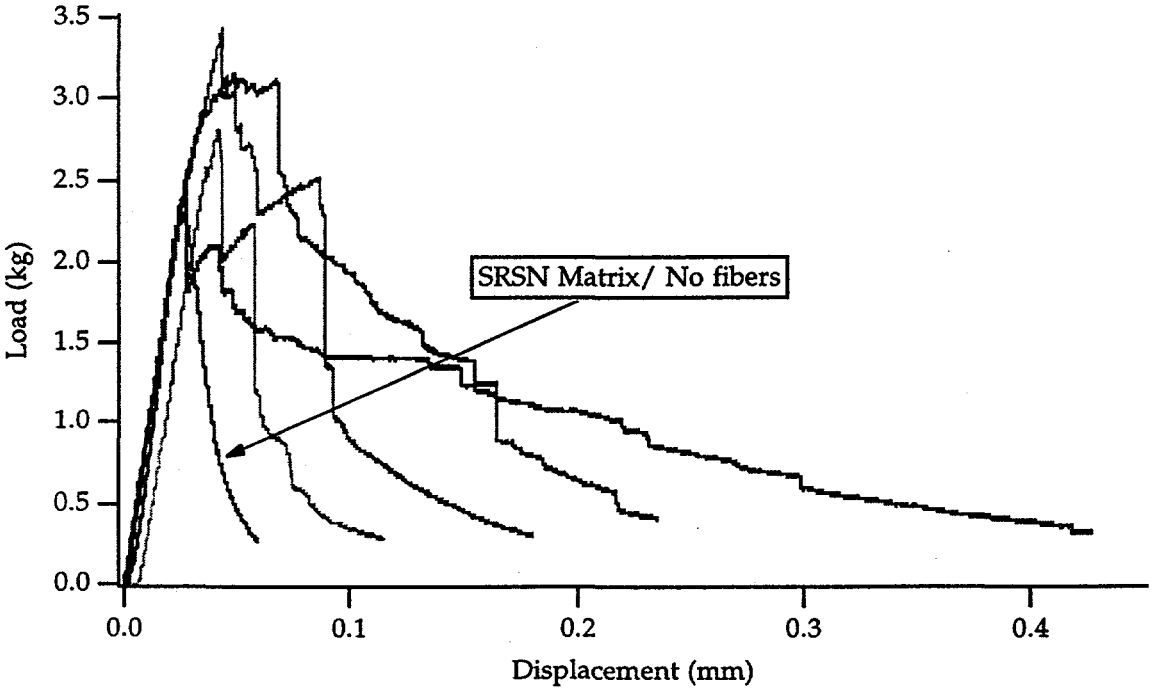

Figure 39. Load-Displacement curve for SRSN composite made with ZrC coated NICALON fiber.

processes are optimized for an individual system, these variations should be significantly reduced. While gaining this experience is outside of the scope of this project, the assumption can be made that the properties of future composites will be more like the best made in the current experiments.

Figure 40 shows the load-displacement curves for the best composite made and for the matrix alone. A comparison of the work of fracture reveals an eight fold increase for the composite compared to the monolithic material. While work of fracture cannot be directly converted to fracture toughness in non-linear elastic systems, the two are proportionate to each other. So, a significant increase in toughness can be obtained in this system compared to the monolithic material. However, as with the case of the TiN coatings, this system has not been optimized, and properties would be expected to increase even further as an understanding of the system is further developed.

The increase in work of fracture in this system can be attributed to both increased fiber pullout lengths and an overall change in the fracture mechanism for this material. Figures 41 and 42 show fracture surfaces of an un-coated NICALON fiber composite and a ZrC coated NICALON composite,

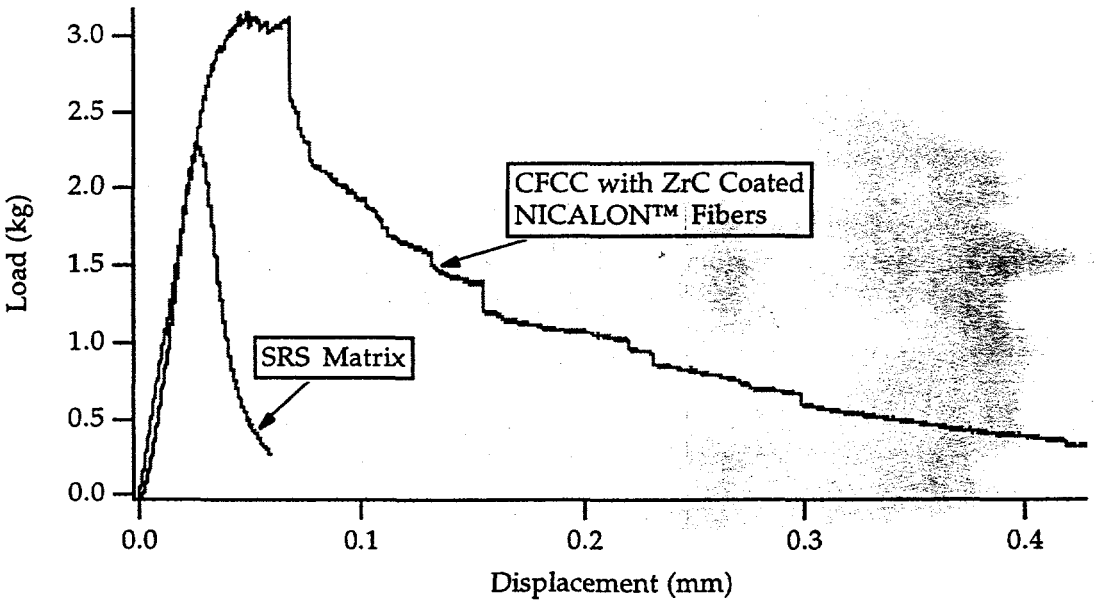

Figure 40. Load-displacement curve for best composite specimen prepared.

respectively. Clearly, the tortuous nature of the crack propagation in the ZrC system has affected the overall load-displacement behavior observed. However, closer examination of the composite shows that this fracture path has been generated due to relief at fiber/matrix interfaces. Figure 43 is a higher magnification image and shows the stepped nature of the fracture path as cracks encounter fiber bundles that have not been fully infiltrated by the matrix material.

Fortunately, regions also exist where matrix infiltration has been successful. In these regions, fiber pullout occurs with pullout lengths on the order of 100-150 μm. While these pullout lengths are still smaller than desired, they do provide for the increased toughness observed in this system. However, unlike the TiN system, this system shows extensive chemical activity during densification. In fact, this system could best be described as containing a reactive interface.

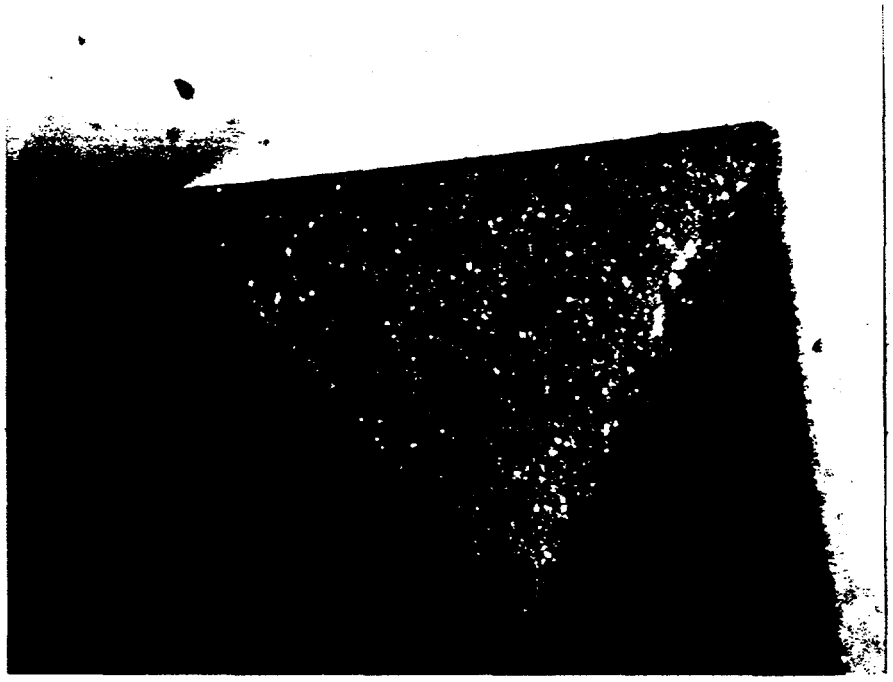

Figure 41. Fracture surface of composite prepared with un-coated NICALON fibers.

Figure 42. Fracture surface of composite prepared with ZrC coated NICALON fibers.

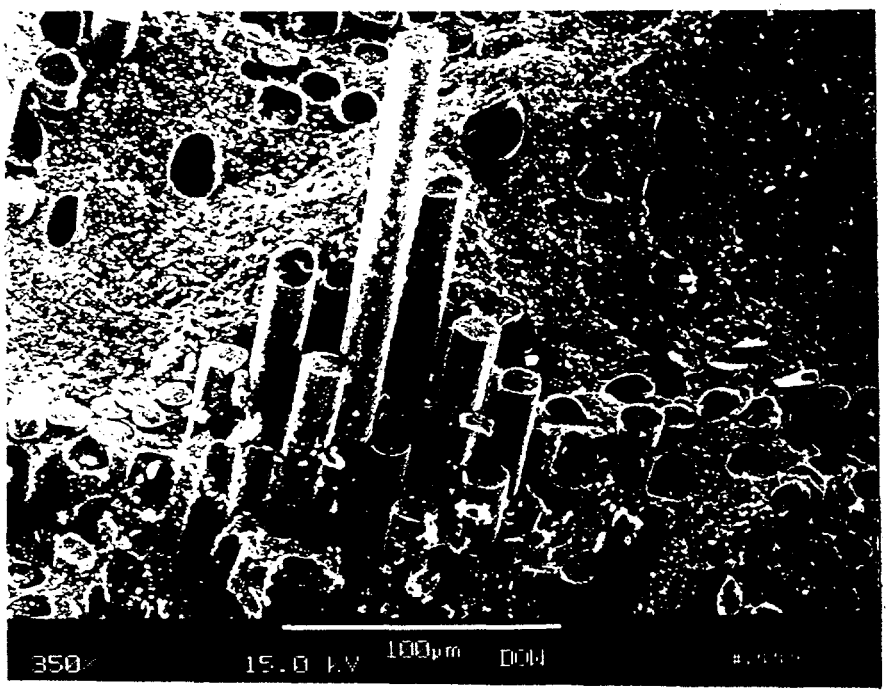

Figure 43. Fracture surface of composite prepared with ZrC coated NICALON fibers.

Two types of coatings were seen in the ZrC coated NICALON fibers. Figures 44 and 45 show representative micrographs of these fibers. The coating type represented in Figure 44 averages 750Å in thickness and fully covers the fiber surface. The coating type represented in Figure 45 averages 2000Å in thickness and also fully covers the fiber surface. Within a typical fiber tow, the type of coating seen on an individual fiber changes from a mix of the two types on the outside of the tow to primarily the type shown in Figure 44 at the inside of the tow. However, this variation is not significant.

What is significant is the chemical reactivity of the coating. Analytical transmission electron microscopy (ATEM) results show that the coatings are made up of a mixture of fine grained cubic ZrC and monoclinic ZrO_2. Figure 46 shows a micrograph of a composite made with these fibers after densification. The dark region at the interface between the fiber and matrix has been identified by ATEM to be a thin (ca. 400Å) crystalline graphite coating (see Figure 47). As mentioned in the introductory section, carbon interfaces, while providing desirable interface properties, are extremely difficult to obtain because of reactivity during processing. In this case, however, the carbon interface has been obtained via a reaction at the interface.

Thermodynamic calculations for this system show that the stable phases under equilibrium conditions are ZrN and ZrO_2. Consequently ZrC would be expected to react with either nitrogen or oxygen in the system to produce the equilibrium species. Carbon would also be a product of the reaction. It is possible that this carbon has been left at the interface as a reaction product, while the zirconium containing species have diffused away. This theorem is supported by the heavy presence of a Zr rich species in the fibers themselves. Figure 48 shows a back scattered electron micrograph of this composite. The dark region at the core of the fibers is an area rich in magnesium. This has most likely diffused from the MgO present in the glassy phase of the matrix. Just outside of this is the bright region which is rich in zirconium. In contrast to this, the regions in the fiber and matrix near the interface are deplete of any zirconium species. It is possible that intercalation of a zirconium species into the structure of the fiber has stabilized the fiber from

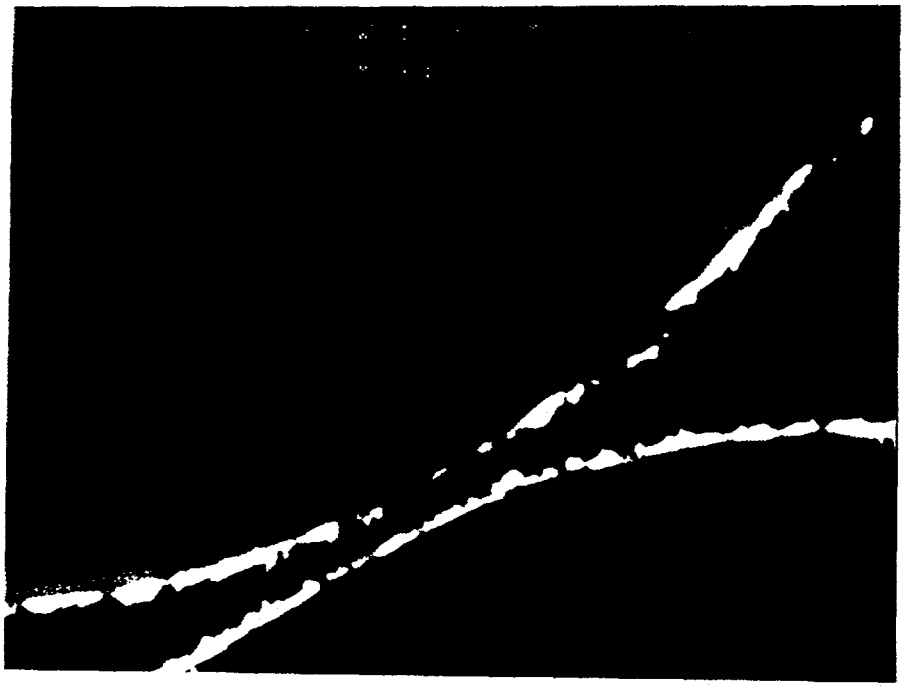

Figure 44. Scanning electron micrograph of as-received ZrC coated NICALON fiber (interior of fiber tow).

Figure 45. Scanning electron micrograph of as-received ZrC coated NICALON fiber (exterior of fiber tow).

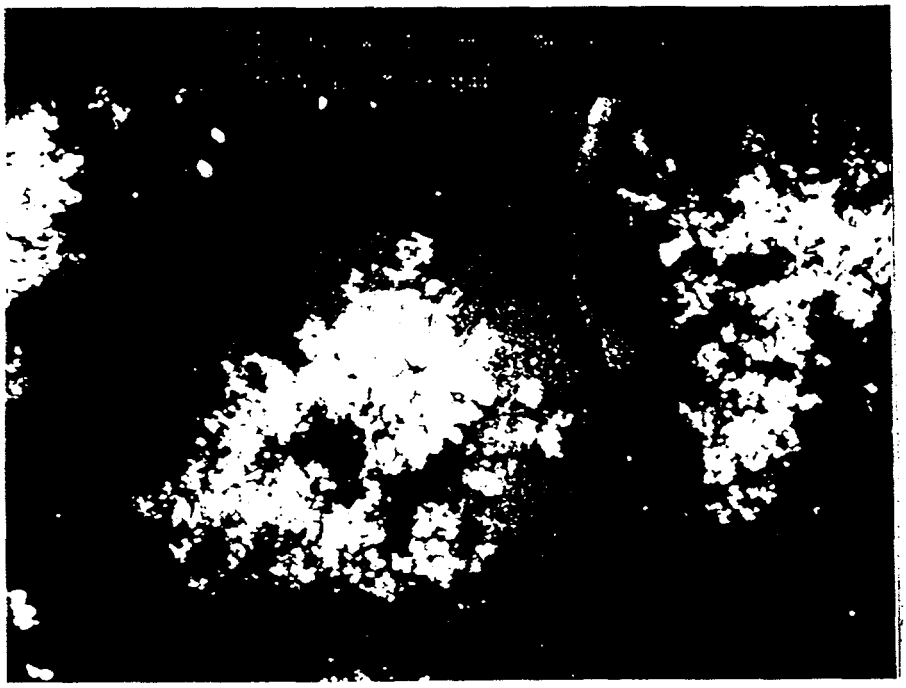

Figure 46. Polished cross section of densified composite prepared with ZrC coated NICALON fibers.

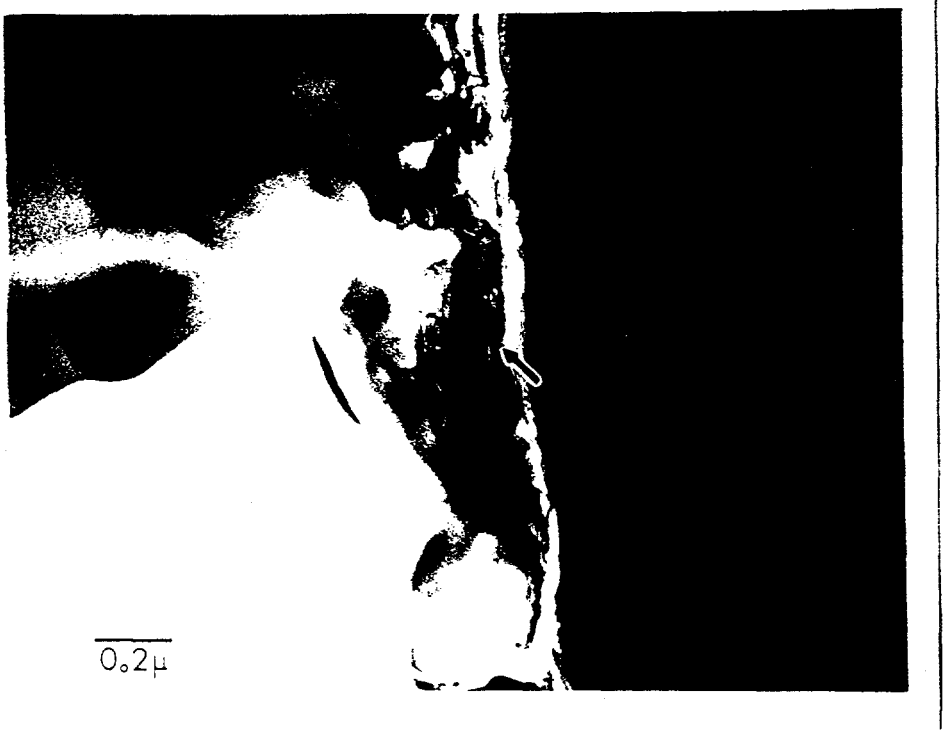

Figure 47. Transmission electron micrograph of NICALON fiber/SRSN interface. Graphite interface shown at arrow.

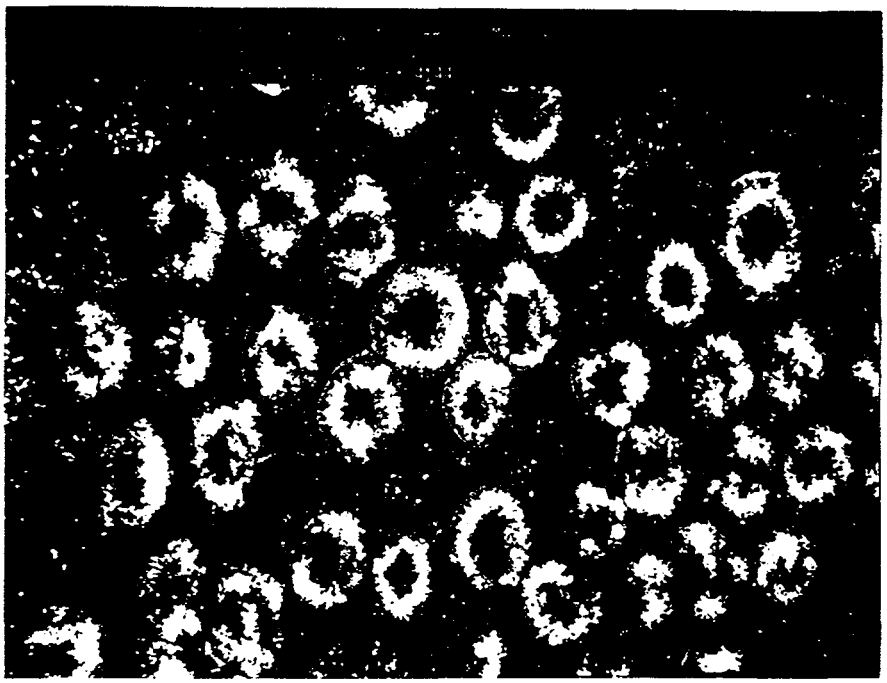

Figure 48. Back scattered electron micrograph of composite prepared with ZrC coated NICALON fibers.

the grain growth seen with other coatings. However, no empirical data exists to support this theorem.

Nevertheless, this unique system has been shown to dramatically improve the toughness in the NICALON fiber SRSN composite system. However, these properties have been measured at room temperature only. The stability of this graphitic interface at elevated temperatures during in-service use is still in question.

Comment on fiber coating quality:

Fiber coatings which were received from Dow's primary fiber coating supplier have been analyzed and found, in many instances, to be inadequate. Complete coverage of fibers with the coatings was often not achieved, and leaves the interpretation of mechanical properties of composites open to the

possibility that partial bonding in these systems may have occurred. Based on analysis of as-received coated fibers and composites prepared with these fibers, it was decided to repeat the property evaluation of several coatings which showed evidence of limited fiber pullout. These coatings are currently being applied to NICALON fibers, TYRANNO fibers and HPZ fibers by a secondary supplier and will be tested as they become available. With the exception of the ZrC coatings, it is anticipated that new interfacial coatings will not be reactively formed during processing. Consequently, these systems would be expected to have higher temperature stability than the ZrC system.

As was mentioned previously, the properties of these composites can be affected by both fiber coatings and the properties of the fiber itself. In general, this study found that composites prepared with NICALON fibers showed the best mechanical properties, independent of the fiber coating used. Composites prepared with TYRANNO fibers showed slightly poorer properties than the NICALON fiber composites and composites prepared with NEXTEL™ 550 fiber were even poorer yet. This behavior is not unexpected since the NEXTEL™ fibers are oxide based and the matrix is non-oxide based. In addition, higher fiber strength degradation in TYRANNO fibers is expected compared to NICALON fibers because of the higher levels of SiO_2 and carbon present in these fibers. Once again, fibers such as HPZ fibers or stoichiometric SiC fibers would be expected to perform even better than the NICALON fibers because of their higher temperature stability.

VII. APPLICATION TESTING

A. Introduction

The results described above are for testing of materials at room temperature or at elevated temperature in an air environment. However, testing in environments which are representative of the actual application environment has provided more detailed data concerning the performance of these CFCC's.

In conventional ethylene manufacturing technology, the primary reaction is thermal pyrolysis or cracking. In this process, hydrocarbon feed is mixed with diluent steam and then heated to > 800°C for a period typically less than one second. One of the undesirable side reactions which occurs in this process creates several forms of carbonaceous materials known collectively as coke. Build-up of coke on reactor walls can lead to a variety of problems, including reduced yield and reactor tube failure. For this reason, reactor tubes are periodically burned out to remove excess coke. This process is time consuming and costly. Consequently, a strong driving force exists for reducing the extent of coke formation.

While the mechanisms of coke formation are complex, in simple terms, a form of coke known as catalytic coke is initially formed on the reactor walls followed by build-up of additional forms of coke on the surface of the freshly created catalytic coke. Formation of catalytic coke is known to be enhanced by the presence of certain metal components that are used in typical reactor tubes. These alloys are necessary to maintain the mechanical integrity of the tube under thermal and vibrational cycles which occur during operation. Previous to this study, it was postulated that the use of a CFCC reactor tube could reduce the formation of catalytic coke, while at the same time maintain the requisite mechanical integrity. The environmental evaluation portion of this program was designed to determine the merit of this concept.

Specifically, the exposure tests conducted in this study have helped to define the compatibility of the material system which Dow has chosen and the application environment. This interaction is critical from several different view points. First, gas chromatography (GC) has been used to determine if the presence of the CFCC material has an effect on the reaction products. It was anticipated that the presence of a ceramic material would not be detrimental to the ethylene yield from this type of cracking operation. However, it was critical to ensure that this was true. Secondly, this testing has provided critical information concerning coke formation and build up, corrosion and erosion, and thermal shock of Dow's CFCC material.

B. Experimental Procedure

Independent of this program, Dow has designed and constructed two lab scale evaluation rigs to perform environmental testing. These rigs were designed to crack hydrocarbon feed stock under similar conditions to that used in production (e.g. feed stock, steam/hydrocarbon ratio, feed rates). As a performance benchmark, HP-40 tubes were obtained and installed for these rigs. HP-40 is the alloy currently used in Dow's production facilities.

Since this work was concurrent with the process development work being conducted on the CFCC material, testing was originally done using small CFCC samples. In this case, CFCC specimens were prepared using the tape casting method described in previous sections. No fiber coating was used since this would be expected to affect chemical interactions between the process environment and the specimen, and fiber coating work was incomplete at the time of testing. Specimens were approximately 6 mm cubes and were suspended in the hot zone of HP-40 tubes.

Testing was also done on monolithic ceramic tubes. The ceramic tubes examined in this study were 99.5% Al_2O_3 (Coors Ceramics) and silicon nitride (Ceradyne). The dimensions for these tubes were identical to that of the standard HP-40 tubes. To insure the residence time in the tube was similar to that used in production (<1 second), it was necessary to insert a quartz rod in both the ceramic and metal tubes. By doing so, the residence time could be reduced to 0.5 seconds for a reasonable hydrocarbon feed flow rate. Since the presence of sulfur is known to decrease the extent of coke formation in metallic tubes and is commonly used in commercial operations, testing was also conducted for all tubes in the presence of CS_2.

To determine the relative coking rates, specimen weights were recorded after one, three and five days of exposure. Specimens were then evaluated via optical and SEM microscopy, energy dispersive spectroscopy (EDS), and wave dispersive spectroscopy (WDS). In the case of the tubular specimens, a boroscope was used to examine the coke inside the tube prior to further evaluation.

C. Results and Discussion

As discussed above, a process to manufacture tubular CFCC's was still being developed during the period of environmental exposure analysis. This necessitated the use of small CFCC coupons which were suspended in the process stream. However, the presence of the coupon itself can affect the temperature profile in the tube and the residence time of the feed stock. So, while the effect of exposure to the process environment could be qualitatively examined by suspending coupons in the process stream, meaningful quantifiable results were difficult to obtain.

Since the surface of a CFCC component is likely to consist primarily of the matrix material, coke formation is speculated to be dominated by the chemistry of the matrix rather than the fibers. In addition, since the presence of coupons in the process stream created difficulties in simulating the process environment, tubes made from the matrix material, silicon nitride, were used to generate quantifiable data.

However, for cost considerations, initial testing to establish appropriate test procedures was conducted using less expensive Al_2O_3 tubes. Results for the Al_2O_3 tubes run without CS_2 is shown below:

Run #	Time(hrs)	Coke Formed (g)	g/hr
1	24	9	0.38
2	24	9	0.38
3	24	14	0.57
4	72	6	0.08
5	120	27	0.23
6	120	45	0.38

This data, while showing considerable scatter, was useful for indicating the improvements (including a more accurate weighing system) which were necessary to obtain accurate data for the silicon nitride tubes.

Figure 49 shows a comparison of the weight gain due to coking as a function of time for the silicon nitride tube and the HP-40 tube that were run in the presence of CS_2. Results indicate that in both cases, coke formation is rapidly

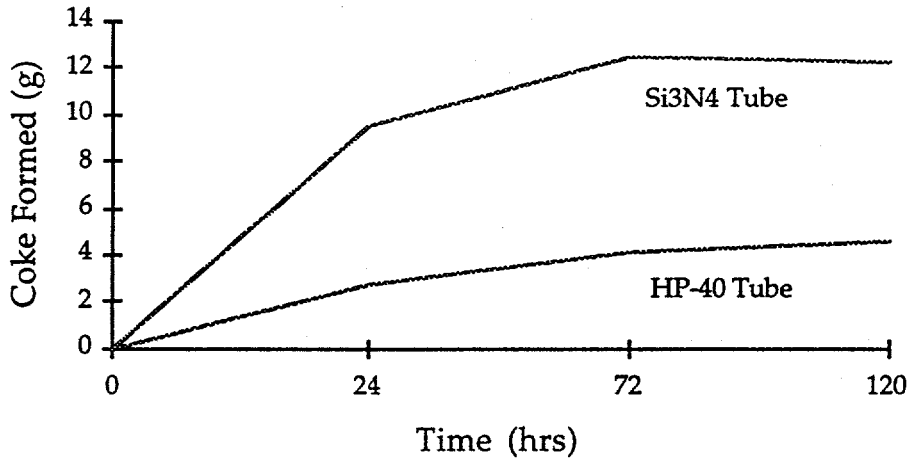

Figure 49. Coke formation as a function of time for HP-40 and Si_3N_4 tubes.

developed and then appears to slow as time continues. In addition, the relative coke formation is lower for the HP-40 tube than for the silicon nitride tube. However, since the CS_2 is typically used to passivate the surface of the metallic tube to minimize coke formation, it would most likely not be used with a CFCC replacement tube. A comparison of the coke formation for the HP-40 and two silicon nitride tubes with and without CS_2 after 72 hours exposure is shown below:

Tube	CS_2?	Coke Formed (g)	g/hr
HP-40	Yes	4.08	0.06
Si_3N_4	Yes	12.47	0.17
HP-40	No	61.23	0.85
Si_3N_4 (#1)	No	5.22	0.07
Si_3N_4 (#2)	No	5.00	0.07

As can be seen, the coke formation for the HP-40 tubes is dramatically reduced in the presence of the CS_2. However, a comparison of the coke

formation for the silicon nitride without CS_2 and the HP-40 tube with CS_2, shows that the relative coking rates are nearly identical.

Boroscopic examination of the tubes showed that, in general, coke deposits were minor at the tube entries and increased in amount with the length of the tube, as expected. The coke produced in the end of the silicon nitride tube was generally softer than that from the end of the metallic tube, while that coke in the middle of the tubes was similar in appearance for both tubes.

Flakes of coke were taken from these tubes and analyzed to determine if a difference in the type of coking could be seen. Flakes were taken from the Si_3N_4 tube from the outer surface of the coke (process stream side) and from the inner surface of the coke (tube side). Flakes from the process fluid side were mirror-like and were determined to be a form of coke created by a non-catalytic homogeneous mechanism, i.e. formation of a non-volatile liquid "tar" in the gas phase followed by surface deposition and further dehydrogenation. The mirror finish is thought to be the type formed when the tars are non-viscous liquids which smoothly wet the tube surface prior to dehydrogenation into coke (38). Flakes from the tube side were composed of interconnected spheres laying on a smooth surface. This morphology is often seen and is known as spherical or globular coke (38-39). It is formed by the same mechanism as mirror coke, except that the tar droplets are thought to be too viscous to wet the surface and tend to coagulate. While the majority of the coke found was of the globular type, isolated clusters of coke deposits containing cylindrical structures were also found. This is most likely a form of filamentous coke that is catalytic in nature and is often referred to as "match coke" (40-42).

Flakes taken from both the process fluid side and tube side of the HP-40 tubes showed classic globular coke. Based on this, it would appear that there are no appreciable differences in the type of coke formed in the silicon nitride tubes compared to HP-40 tubes.

Since the original assumption made during the economic evaluation was that a five fold reduction in coke formation would be needed to make the

replacement of the metallic tube with a CFCC tube viable, the data above would suggest that a silicon nitride based CFCC will not meet the acceptance criteria.

This conclusion is further supported by the data generated from the CFCC coupons that were exposed to the process environment. Microscopic examination of these coupons showed evidence of chemical attack at the surface. This attack was concentrated on the glassy phase which is added to Si_3N_4 to enhance the sinterability. Under the low oxygen partial pressures which exist in a cracking operation, this glassy phase can undergo a reduction reaction to form gaseous by-products. Under these conditions, corrosion of the inner tube wall would occur continually until failure occurred. These results would indicate that a decrease in the lifetime of the tube compared to current HP-40 tubes would result. Combining this undesirable outcome with the results concerning coke formation leads to the inevitable conclusion that a silicon nitride based CFCC will not be a viable option in this application.

Of course, this leads to the question of what materials would be viable. Unlike Si_3N_4 which must contain a glassy phase for the densification process, SiC typically does not. Silicon carbide, which has been explored in the heat exchanger industry (43), has several advantages. First, while it typically has an oxide surface, once this surface is removed, it is not likely for further reactions to occur in an environment with low partial pressures of oxygen such as in a cracking furnace. Silicon carbide also has the advantage of having a high thermal conductivity and could thus provide for good heat transfer. However, SiC has inherently poor toughness and would be difficult to design into a reactor tube of the dimensions needed here. Use of a fiber reinforced SiC composite could solve this issue. Unfortunately, as was discussed previously, the techniques which have been developed for manufacturing these composites have not yet reached a point where gas impermeable tubes can be formed.

VIII. CONCLUSIONS

A comparison of the state of Dow's CFCC technology prior to the beginning of this cooperative agreement and its current state is summarized below:

Prior to cooperative agreement:

- Inhomogeneous infiltration of matrix into fiber tows.
- Insufficient strength in tapes to handle during lamination steps.
- Insufficient flexibility in tapes to make tubular components. Only flat plates could be made with this process.
- Only limited work done on interfacial modifications. No improvements in properties were observed.
- Understanding of temperature limitation of fibers restricted to literature.
- Ability to make fully dense composites restricted to flat plate shapes via hot pressing at 1825°C.

Current Status:

- Good matrix infiltration into fiber tows.
- Improved strength of tapes through modification to chemistry and casting procedures.
- Flexibility of tapes improved to the point where tubes as small as 2" in diameter can be made.
- Processing procedures developed to make tubes as long as 12 inches.
- Temperature limitations for various commercially available fibers have been established.
- Pressureless and pressure-assisted densification processes have been explored. Full density in composites has been achieved at 1600°C under isostatic conditions.
- Fiber coatings have been screened for NICALON, TYRANNO, and NEXTEL™ 550 fibers. A coating has been identified for

NICALON fiber composites which shows an 8x improvement in the work of fracture compared to the monolithic silicon nitride matrix.

Despite the improvements in processing and material properties, environmental exposure tests showed that Dow's target matrix material was not compatible with the process environment for the application. Further development of processing techniques for this material system will need to be focused toward other applications.

IX. APPENDIX A

TASK 1 APPLICATION ASSESSMENT

1.1 Analysis

1.1.1 Establish the criteria for redesign of components and systems.

1.1.2 Perform an energy impact study on the use of CFCC's in the production of ethylene. For this study, SRI International's Process Economics Program report 29E will be used as the source of information concerning ethylene production facilities. All changes to systems and processes will be referenced to SRI's standard ethylene plant.

1.2 Definition

1.2.1 A matrix material has already been chosen based on it's performance as a monolithic material. The chosen matrix will be one of a class of materials known as self reinforced silicon nitride (SRSN). These materials were developed at Dow and show improved properties over standard silicon nitride.

1.2.2 Evaluation of available processing routes has already been accomplished. Although tape casting has been chosen as one of the most promising techniques, the processing routes to be explored may not be limited to tape casting only. For instance, pressure filtration and/or use of tape casting technology in filament winding processes may be secondary routes explored at later stages of the program.

1.2.3 Determine the performance requirements for the application and the expected mechanical properties of the composite material.

1.2.4 Perform an economic evaluation of the tape casting process, the pressure filtration process, and the filament winding process relative to the value of the final components.

1.3 Design Studies

1.3.1 Determine the specific changes in components necessary to utilize CFCC's in the proposed application.

1.3.2 Determine the specific changes in the systems necessary to utilize CFCC's in the proposed application.

1.3.3 Use finite element analysis to determine the principle stresses in the component during operation.

1.3.4 Determine the appropriate fiber architecture for reinforcing the component based on the results of Task 1.3.3.

TASK 3 MATERIALS AND PROCESS DEVELOPMENT

3.1.1 Fiber Optimization

3.1.1.1 Examine candidate fibers which may include but not be limited to NICALON, NEXTEL, and HPZ fibers. Screening of fibers will be done in conjunction with Task 3.1.4 and will be accomplished by manufacturing and testing of composites. For more information, see Task 3.1.4.

3.1.3 Matrix Infiltration/Densification

3.1.3.1 Optimize the tape casting formulations by preparing formulations with varying amounts of plasticizer and binder and examining each formulation's ability to infiltrate a variety of fiber architectures. Because infiltration is expected to become more difficult as the fiber architecture complexity increases, this task may include but not be limited to various satin harnesses and plain weave clothes. Utility of tape formulations will be determined by a variety of techniques including but not limited to viscosity measurements and optical microscopy.

3.1.3.2 Prepare tapes via the tape casting method of uniaxially aligned fibers infiltrated with SRSN.

3.1.3.3 Determine appropriate lamination and binder burnout procedures and address other related intermediate processing step problems.

3.1.3.4 Explore densification of composites. Although hot pressing can be utilized to fully densify these materials, other

techniques need to be examined to address shaped articles which will be required for the chosen application. Processing techniques may include but not be limited to sintering, over-nitrogen pressure sintering, and hot isostatic pressing. Should results indicate a change in composition of the matrix would help to achieve required densities, adjustments in composition will be examined.

3.1.3.5 Based on the results of Task 3.1.3.4, determine if alteration of SRSN composition would be expected to improve densification and, if necessary, repeat experiments with new compositions.

3.1.4 Fiber Coatings

3.1.4.1 Coat 250 meter of NICALON and NEXTEL 550 fiber, and 400 meter of HPZ fiber with a CVD coating. The coatings will most likely be C/TiC, C/TiN, C/SiC, C/TiB_2, C/BN, BN/TiC, BN/TiN, TiB_2/C/BN, and SiC/BN. Microscopy of the coated fibers will be performed as an initial screening for those materials unsuitable for continuation to Task 3.1.4.2.

3.1.4.2 Prepare tapes of uniaxially aligned fiber infiltrated with SRSN for the most promising fibers and coatings. Laminate and hot press these tapes into billets. Hot pressing of these materials, as well as those in Task 3.1.4.5, will be done because appropriate densification techniques from other methods will not yet have been established. In addition, since only simple uniaxial composites will be prepared, hot pressing will be a quick, simple technique for densification.

3.1.4.3 Measure the room temperature properties of the composites. Properties to be measured may include but not be limited to room temperature strength, toughness and an evaluation of the extent of fiber pullout via fractography. These properties will be measured as a comparative test for screening purposes only.

3.1.4.4 Coat additional fiber as determined in Milestone III-4 with three thicknesses of the chosen coating for each fiber. If results of Task 3.1.4.6 indicate that additional coating thicknesses should be explored, coat additional fibers and repeat Tasks 3.1.4.5 and 3.1.4.6

3.1.4.5 Prepare tapes of uniaxially aligned fiber infiltrated with SRSN for each fiber coating. Laminate and hot press these tapes into billets.

3.1.4.6 Measure the room temperature properties of the composites. Properties to be measured may include but not be limited to room temperature strength, toughness and an evaluation of the extent of fiber pullout via fractography.

3.1.4.7 Based on the results of Task 3.1.4.6, choose the most promising fiber/coating system and coat 2.5 lbs of fiber with the appropriate coating.

3.1.4.8 Evaluate the properties of the composites prepared for Milestone III-7. The properties to be measured may include but not be limited to room temperature strength, toughness, hardness, modulus, 0° and 90° abrasion resistance, elevated temperature strength, creep rupture, thermal expansion and thermal conductivity.

3.1.4.9 Perform environmental testing on the composites by placing specimens in simulated end-use application environments. Testing may include but not be limited to corrosion and reactivity.

3.1.4.10 If necessary, surface coat test specimens and evaluate the composite properties. Measured properties may include but not be limited to hardness and abrasion resistance.

3.1.4.11 If necessary, perform environmental testing on the coated composites by placing coated specimens in simulated end-use application environments. Testing may include but not be limited to corrosion and reactivity.

3.1.4.12 Conduct diagnostic non-destructive evaluation of specimens to guide the infiltration and densification studies. Evaluation may include but not be limited to measurement of composite density and porosity

3.1.5 Process Demonstration

3.1.5.1 Based on the results of Task 3.1.3, green process several tubes to be used as demonstration pieces using an appropriate processing technique.

3.1.5.2 Based on the results of Task 3.1.3, densify the tubes by an appropriate technique.

3.1.5.3 Finish machine the tubes.

X. APPENDIX B

A. Process Economics for Tape Casting of CFCC Tubes

This report is intended to be a preliminary assessment of the process economics of manufacturing CFCC's by three processes: tape casting, filament winding, and pressure filtration. The Dow Chemical Company would like to thank SRI, International for the use of information from their process economics program reports.

1. Market Size

One of the first assumptions which must be made during any economic evaluation is that concerning the market size of the product you are proposing to manufacture. For this study, we have used information from SRI, International's Process Economics Program Report 29E. In this report, the world market for ethylene at the end of 1989 was reported to be 60,923,000 tons/year. As this is the most current analysis available to us, we have assumed this market size for our study. According to this report, a standard ethylene plant that has a capacity of 500,000 tons/year uses 6 cracking furnaces plus one spare. This means that to meet the world ethylene market size, 122 plants of this capacity would be required. Although it was not stated in SRI's report, input from Dow personnel with expertise in the area of ethylene production has suggested that approximately 30 cracking tubes are necessary for each cracking furnace. Since each plant has a total of 7 cracking furnaces, a total of 25,620 tubes would be required.

After consultation with Dow's marketing group, it was decided that it would be reasonable to estimate the fraction of tubes replaced by CFCC's would be approximately 40 percent. Dow would conservatively be estimated to capture 25% of this CFCC market. This means that the market size Dow could expect would be 2,562 tubes. However, as each tube is expected to have a life of 5 years, the projected plant capacity for production would be 512 tubes per year.

At this point, it should be noted that there are two reasons why these economics should be considered a preliminary assessment. First, as is shown later in this report, the cost of these components is dominated by the cost of raw materials. Because these costs can be expected to vary with changes in volume usage, the economics for this process should be expected to change with time, becoming more realistic as commercialization is approached. Second, from Dow's perspective, a plant would likely be built around the processing technology. This means that we would pursue numerous components and markets which would be based on this technology. In this way, the plant capacity would reach an acceptable level and the capital costs would be distributed over many different markets instead of just one. Based on these two points, it can be expected that should Dow be successful in Phase I of this program, a more realistic economical evaluation would be performed at a later stage.

2. Cost Basis for Tape Casting Process

It has been assumed in this evaluation that the tubes will be made from a NICALON fiber reinforced-self reinforced silicon nitride (SRSN) material. While actual tube size will depend on the plant design into which the CFCC's are incorporated, for the purposes of this evaluation, an average tube size has been assumed (see below). All costs are based on 1992 dollars and market prices for raw materials. Assumptions concerning the required labor, utilities, waste disposal and maintenance were based on the flow diagram shown in Figure B1. Direct fixed costs (DFC) and inventory costs were also calculated based on this diagram. Other costs, such as taxes, depreciation, research costs and selling costs, were based on information from similar size plants currently in place at Dow.

Tube size: 9.1 m X 10.16cm (ID) X 10.795 cm (OD) with 61cm outer radius hairpin

Raw material costs:

Material	Unit Cost($)
Solvent	2.89/liter
Binder	16.94/kg
Surfactant	6.6/kg
Plasticizer	16.94/kg
Mylar	100/roll
Fiber	660/kg
SRSN	70/kg
Coatings	1000/kg of fiber

Labor:

# Salaried Employees	11
# Shift Employees	42

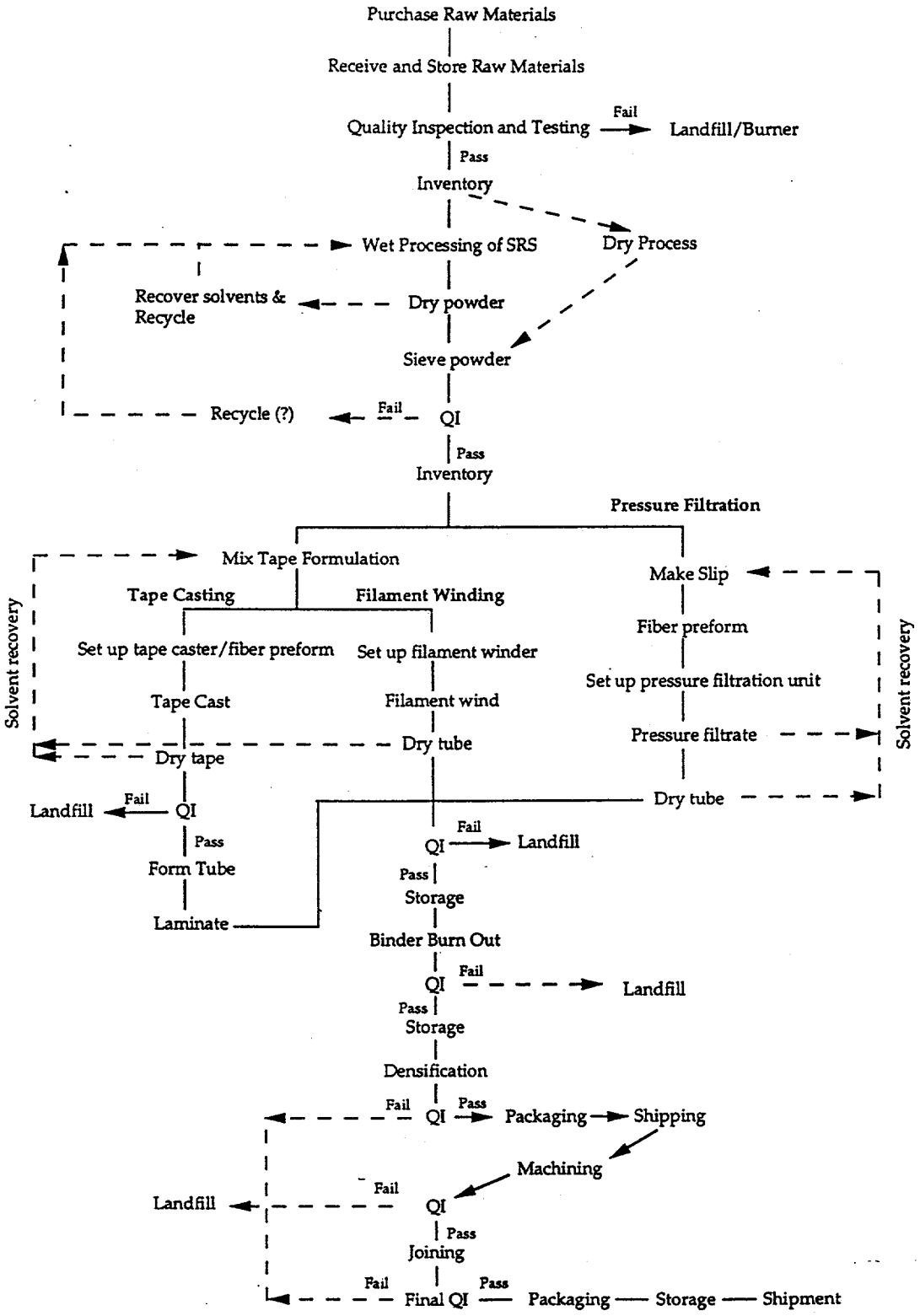

Figure B1. Process Flow Diagram

3. Preliminary Economics

The preliminary economics for the manufacture of CFCC tubes via a tape casting process are shown in Table BI.

	Cost Estimate $/Tube	Capital Cost $/Unit/Yr
Fiber	53,261.99	0
Fiber Coatings	80,700.00	0
All Other Materials	11,975.51	0
Total R.M.	145,937.50	0
Labor, Utilities, Waste Disposal, Maintenance	8,511.72	0
Overhead, Depreciation, DFC,Taxes	5,304.89	34,646.95
R.M. Inventory	0	6,440.45
In-Process Inventory	0	1,209.57
Transfer Inventory	0	2,456.99
Total Bulk	159,754.11	45,753.96
Packaging	1,000.00	0
Total Plant	160,754.11	45,753.96
Selling, Gen. & Adm., Research, Cash & Acc.	18,286.02	37,862.21
Inventory for Sale	0	12,934.95
Total Cost per Tube	203,177.94	96,551.12

Table BI. Preliminary Process Economics for Tape Casting of CFCC Tubes.

B. Alternative Processing Methods For CFCC Tubes

Tables BII and BIII show the results of the economic evaluation for the filament winding and pressure filtration processes. While there are differences in some of the capital costs and labor, the front and back end of these processes are identical to that for the tape casting process. Consequently, the final costs per tube for both of these processes are close to that for the tape casting process. Figure B2 shows the raw material sensitivity plot for the filament winding process. The sensitivity for the pressure filtration process is indistinguishable from that of Figure B2. As with the tape casting processes, the cost of fibers and fiber coatings is dominant.

	Cost Estimate $/Tube	Capital Cost $/Unit/Yr
Fiber	60,460.72	0
Fiber Coatings	91,607.16	0
All Other Materials	13,254.78	0
Total R.M.	165,322.66	0
Labor, Utilities, Waste Disposal, Maintenance	8,963.75	0
Overhead, Depreciation, DFC,Taxes	6,021.91	35,646.94
R.M. Inventory	0	6,428.17
In-Process Inventory	0	1,205.43
Transfer Inventory	0	2,447.02
Total Bulk	180,308.32	45,727.56
Packaging	1,135.16	0
Total Plant	181,443.48	45,727.56
Selling, Gen. & Adm., Research, Cash & Acc.	20,646.33	37,659.44
Inventory for Sale	0	12,859.82
Total Cost per Tube	202,089.81	96,246.82
	202,089.81	96,246.82

Table BII. Preliminary Process Economics for Filament Winding of CFCC Tubes.

	Cost Estimate $/Tube	Capital Cost $/Unit/Yr
Fiber	60,629.60	0
Fiber Coatings	91,863.05	0
All Other Materials	13,047.75	0
Total R.M.	165,540.40	0
Labor, Utilities, Waste Disposal, Maintenance	9,086.61	0
Overhead, Depreciation, DFC,Taxes	6,422.65	37,913.53
R.M. Inventory	0	6,419.35
In-Process Inventory	0	1,203.06
Transfer Inventory	0	2,443.44
Total Bulk	181,049.66	47,979.38
Packaging	1,138.33	0
Total Plant	182,187.99	47,979.38
Selling, Gen. & Adm., Research, Cash & Acc.	20,795.56	37,825.98
Inventory for Sale	0	12,859.32
Total Cost per Tube	202,983.55	98,664.68
	202,983.55	98,664.68

Table BIII. Preliminary Process Economics for Pressure Filtration of CFCC Tubes.

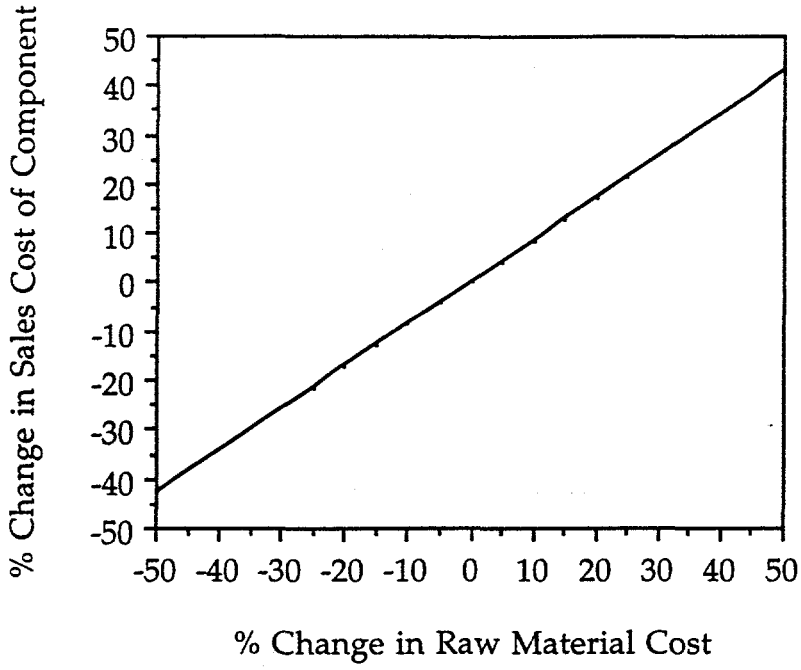

Figure B2. Raw material sensitivity for filament winding process.

X. APPENDIX C

Fabrication Method	Matrix Composition	Fiber Type	Binder Removal Method	Crucible Type	Max. Temp. (°C)	Pressure (atm)	Time (hrs)	Fired Density (g/cc)	% Theoretical Density
Cast	SN-A	None	Air BO	G	1600	10	12	2.684	82.8
Cast	SN-A	None	Air BO	V	1600	10	1	2.692	83.1
Cast	SN-A	None	Air BO	BN	1600	10	12	2.667	82.3
Cast	SN-A	None	Air BO	BN	1600	10	12	2.690	83.0
Cast	SN-A	None	Air BO	BN	1700	10	12	3.124	96.4
Cast	SN-A	None	Air BO	BN	1700	10	12	3.177	98.1
Cast	SN-A	None	Air BO	BN	1600	100	1.5	2.358	72.8
Cast	SN-A	None	Air BO	BN	1600	100	12	2.932	90.5
Cast	SN-A	None	Air BO	BN	1600	100	12	3.222	99.4
Cast	SN-A	None	Air BO	V+G	1600	2000	1	2.661	82.1
Cast	SN-A	None	Air BO	V	1700	2000	1	2.810	86.7
Dry Pressed	SN-A	None	None	BN	1600	10	12	3.025	93.4
Dry Pressed	SN-A	None	None	G	1600	10	12	2.960	91.4
Dry Pressed	SN-A	None	None	G	1600	10	12	2.948	91.0
Dry Pressed	SN-A	None	None	BN	1600	10	12	2.973	91.8
Dry Pressed	SN-A	None	None	BN	1600	10	12	3.009	92.9
Dry Pressed	SN-A	None	None	BN	1750	10	12	3.217	99.3
Dry Pressed	SN-A	None	None	BN	1600	100	1.5	2.601	80.3
Dry Pressed	SN-A	None	None	BN	1600	100	12	3.156	97.4
Dry Pressed	SN-A	None	Air BO	V	1600	2000	1	2.842	87.7
Cast	SN-A	NICALON	Air BO	G	1600	10	12	0.800	26.1
Cast	SN-A	NICALON	Air BO	G	1600	10	12	1.026	33.4
Cast	SN-A	NICALON	Air BO	G	1600	10	12	0.869	28.3
Cast	SN-A	NICALON	Air BO	BN	1600	10	12	0.828	27.0
Cast	SN-A	NICALON	HIP	BN	1825	10	1	2.847	92.8

Fabrication Method	Matrix Composition	Fiber Type	Binder Removal Method	Crucible Type	Max. Temp. (°C)	Pressure (atm)	Time (hrs)	Fired Density (g/cc)	% Theoretical Density
Cast	SN-A	NICALON	Pre-Sint.	BN+G	1600	34	18	2.870	93.6
Cast	SN-A	NICALON	Hot Pressed	BN+G	1600	34	18	2.030	66.2
Cast	SN-A	NICALON	Air BO	BN	1600	100	1.5	0.793	25.9
Cast	SN-A	NICALON	Air BO	BN	1600	100	12	0.569	18.5
Cast	SN-A	NICALON	Air BO	V+G	1600	100	12	2.926	95.4
Cast	SN-A	NICALON	Air BO	VBN	1600	100	12	2.888	94.1
Cast	SN-A	NICALON	Air BO	VBN+G	1600	100	15	2.674	87.2
Cast	SN-A	NICALON	Air BO	V+G	1550	2000	1	2.644	86.2
Cast	SN-A	NICALON	Air BO	V	1600	2000	1	2.979	97.1
Cast	SN-A	NICALON	Air BO	V	1600	2000	1	2.282	74.4
Cast	SN-A	NICALON	Air BO	V	1600	2000	1	Cracked	N/A
Cast	SN-A	NICALON	Air BO	V	1600	2000	1	2.896	94.4
Cast	SN-A	NICALON	Air BO	V	1600	2000	1	Cracked	N/A
Cast	SN-A	NICALON	Air BO	V	1600	2000	1	No seal	N/A
Cast	SN-A	NICALON	Air BO	V	1700	2000	1	2.053	66.9
Cast	SN-A	HPZ	Air BO	G	1600	100	12	0.900	29.3
Cast	SN-A	HPZ	Air BO	V+G	1600	2000	1	3.178	103.5
Cast	SN-A	NICALON	Air BO	Hot Pressed	1600	340	1	2.260	73.7
Cast	SN-A	NICALON	Air BO	Hot Pressed	1825	340	1	3.060	99.8
Cast	SN-C	None	Air BO	G	1600	10	12	2.718	
Cast	SN-C	None	Air BO	G	1600	10	12	1.009	
Dry Pressed	SN-C	None	None	G	1600	10	12	2.931	
Dry Pressed	SN-C	None	None	BN	1600	10	12	2.998	
Cast	SN-B	None	Air BO	BN	1600	10	12	2.871	88.6
Cast	SN-B	None	Air BO	BN	1600	10	12	2.775	85.6

Fabrication Method	Matrix Composition	Fiber Type	Binder Removal Method	Crucible Type	Max. Temp. (°C)	Pressure (atm)	Time (hrs)	Fired Density (g/cc)	% Theoretical Density
Cast	SN-B	None	Air BO	G	1600	10	12	2.620	80.9
Cast	SN-B	None	Air BO	BN	1650	10	12	3.149	97.2
Cast	SN-B	None	Air BO	BN	1700	10	12	2.906	89.7
Cast	SN-B	None	Air BO	BN	1700	10	12	2.813	86.8
Cast	SN-B	None	Air BO	BN	1700	10	12	3.219	99.4
Cast	SN-B	None	Air BO	BN	1700	10	12	3.220	99.4
Cast	SN-B	None	Air BO	G	1750	10	12	3.151	97.3
Cast	SN-B	None	Air BO	BN	1750	10	12	3.120	96.3
Cast	SN-B	None	Air BO	BN	1750	10	12	3.210	99.1
Cast	SN-B	None	Air BO	BN	1600	100	1.5	1.878	58.0
Cast	SN-B	None	Air BO	BN	1600	100	12	3.007	92.8
Dry Pressed	SN-B	None	None	BN	1600	10	12	2.880	88.9
Dry Pressed	SN-B	None	None	G	1600	10	12	2.774	85.6
Dry Pressed	SN-B	None	None	BN	1600	10	12	2.938	90.7
Dry Pressed	SN-B	None	None	BN	1650	10	12	3.023	93.3
Dry Pressed	SN-B	None	None	BN	1700	10	12	3.229	99.7
Dry Pressed	SN-B	None	None	BN	1700	10	12	3.238	99.9
Dry Pressed	SN-B	None	None	BN	1750	10	12	3.175	98.0
Dry Pressed	SN-B	None	None	G	1750	10	12	3.176	98.0
Dry Pressed	SN-B	None	None	BN	1750	10	12	2.239	69.1
Dry Pressed	SN-B	None	None	BN	1600	100	1.5	2.156	66.5
Dry Pressed	SN-B	None	None	BN	1600	100	12	2.958	91.3
Cast	SN-B	NICALON	Air BO	V	1600	10	1	2.084	67.9
Cast	SN-B	NICALON	Air BO	BN	1600	10	12	1.100	35.9
Cast	SN-B	NICALON	Air BO	G	1600	10	12	1.600	52.2

Fabrication Method	Matrix Composition	Fiber Type	Binder Removal Method	Crucible Type	Max. Temp. (°C)	Pressure (atm)	Time (hrs)	Fired Density (g/cc)	% Theoretical Density
Cast	SN-B	NICALON	Air BO	BN	1650	10	12	0.900	29.3
Cast	SN-B	NICALON	Air BO	BN	1700	10	12	0.900	29.3
Cast	SN-B	NICALON	Air BO	BN	1700	10	12	0.900	29.3
Cast	SN-B	NICALON	Air BO	BN	1750	10	12	1.463	47.7
Cast	SN-B	NICALON	Air BO	G	1750	10	12	1.300	42.4
Cast	SN-B	NICALON	Air BO	BN	1750	10	12	0.800	26.1
Cast	SN-B	NICALON	Air BO	BN	1600	100	1.5	1.100	35.9
Cast	SN-B	NICALON	Air BO	BN	1600	100	12	1.210	39.4
HP	SN-B	NICALON	Hot Pressed	BN	1600	10	12	3.065	99.9
HP	SN-B	NICALON	Hot Pressed	BN	1600	100	1.5	3.074	100.2
HP	SN-B	NICALON	Hot Pressed	BN	1600	100	12	3.059	99.7

XI. REFERENCES

1) H. H. Moeller, W. G. Long, A.J. Caputo, and R. A. Lowden, "SiC Fiber Reinforced SiC Composites Using Chemical Vapor Infiltration," SAMPE Quarterly **17** [3] 1-4 (1986).

2) T. Huynh, C. V. Burkland, B. Bustamante, J. Walcher, and J. Patik, "Fabrication of Ceramic Matrix Composite Turbine Rotor Via CVI-SiC Process," NASA Conference Publication 3133, Part 2, 565-594, (1991).

3) J. Sankar, A.D. Kelkar, and R. Vaidyanathan, "Investigation of Forced and Isothermal Chemical Vapor Infiltrated SiC/SiC Ceramic Matrix Composites," Final Report for U.S. Department of Energy, Report # ORNL/Sub/88-SC423/01, September, (1993).

4) C.G. Pantano, G.L. Messing, D. Qi, and W. Minehan, "Sol/Gel Processing Techniques for Glass Matrix Composites," Air Force Weapons Laboratory Report # AFWL-TN-86-59, (1987).

5) J. Wang, R. Piramoon, C.B. Ponton, and P.M. Marquis, "An Application of Sol Gelation in the Dispersion Mixing of Ceramic-Matrix Composites," J. Mater. Sci. Lett. **11** [12] 807-809 (1992).

6) W.H. Atwell, P. Foley, W.E. Hauth, R.E. Jones, N.R. Langley, and R.M. Salinger, "Advanced Ceramics Based on Polymer Processing - Volume II: Composites Technology," DARPA report # AFWAL-TR-4146, August, (1989).

7) F. I. Hurwitz, "Approaches to Polymer Derived CMC Matrices," 24th Int. SAMPE Tech. Conf. Proc., T950-T958, (1992).

8) M. Parlier, E. Bouillon, C. Muller, B. Bloch, P. Noireaux, and J. Jamet, "Process for the Production of a Ceramic Fiber/Matrix Composite Material," U.S. Patent No. 5,196,235 (1993).

9) L. G. Fritzemeier, "Fabrication Optimization of Candidate Materials and Evaluation of Turbine Blade Root Attachments for SSME Turbopump Turbine Blades," NASA Contractor Report 189123, (1992).

10) B. Thomson and J-F. LeCostaouec, "Recent Developments in SiC Monofilament Reinforced Si_3N_4 Composites," SAMPE Quarterly, 46-51, April, (1991).

11) Y. Deming, Y. Xinfang, and P. Jin, "Continuous Yarn Fibre-Reinforced Aluminum Composites Prepared by the Ultrasonic Liquid Infiltration Method," J. Mat. Sci. Letters, **12** [4] 252-253 (1993).

12) "Fibre Reinforced Silicon Nitride Ceramics," New Materials World, 8, May, (1992).

13) A. Yamakawa, " A Process for the Production of a Fibre or Whisker Reinforced Ceramic Compact," European Patent Application No. 92106058.8, (1992).

14) A.W. Urquhart, "Molten Metals Sire MMCs, CMCs," Advanced Materials and Processes, 25-29, July, (1991).

15) H.D. Lesher, C.R. Kennedy, D.R. White, and A. W. Urquhart, "Method of Making Ceramic Composites," U.S. Patent No. 4,921,818, (1990).

16) C. R. Kennedy and M. S. Newkirk, "Method of making Shaped Ceramic Composites," U.S. Patent No. 5,024,795, (1991).

17) R. K. Dwivedi, "Method of Making Metal Matrix Composites," U.S. Patent No. 4,998,578, (1991).

18) R.E. Mistler, "Tape Casting: The Basic Process for Meeting the Needs of the Electronics Industry," Ceramic Bulletin, **69** [6] 1022-1026 (1990).

19) R.T. Bhatt, "Method of Preparing Fiber Reinforced Ceramic Material," U.S. Patent No. 4,689,188 (1987).

20) R.N. Singh, "Method of Obtaining a Filament Containing Composite With a Boron Nitride Coated Matrix," U.S. Patent No. 4,931,311 (1990).

21) J.E. Grady and B.A. Lerch, "Evaluation of Thermomechanical damage in SiC/Titanium Composites," NASA Conference Publication 10051, 33-1 to 33-14, (1990).

22) M.H. Jaskowiak, M.J. Hyatt, W.H. Philipp, J.I. Eldridge, J.A. Setlock, "Effects of ZrO_2 Interfacial Coatings in Al_2O_3/Al_2O_3 Composites," NASA Conference Publication 10051, 60-1 to 60-12, (1990).

23) A. Bose, J. Lankford, R. Page, and C. Blanchard, "Fiber and Whisker Reinforced Composites and Method for Making Same," U.S. Patent No. 5,166,004 (1992).

24) A.J. Pyzik, W.J. Dubensky, D. B. Schwarz, and D. R. Beamon, "Self-Reinforced Silicon Nitride Ceramics of High Fracture Toughness and a Method of Preparing Same," U.S. Patent No. 4 883 776, (1989).

25) F.J. Frechette, W.D.G. Boecker, C.H. McMurtry, and M.R. Kasprzyk, "Non-Oxide Sintered Ceramic Fibers," U.S. Patent No. 5,135,895, (1992).

26) J. A. DiCarlo, "High Temperature Structural Fibers - Status and Needs," NASA Technical Memorandum 105174, (1991).

27) P. Greil, "Thermodynamic Calculations of Si-C-O Fiber Stability in Ceramic Matrix Composites," J. European Ceram. Soc., **6** 53-64 (1990).

28) M. H. Jaskowiak, "Effects of High Pressure Nitrogen on the Thermal Stability of SiC Fibers," NASA Technical Memorandum 103245, (1991).

29) B.A. Bender, J.S. Wallace, and D.J. Schrodt, "Effect of Thermochemical Treatments on the Strength and Microstructure of SiC Fibers," J. Mater. Sci. **26**, 970-976, (1991).

30) A. Zangvil, Y-W. Chang, N. Finnegan, and J. Lipowitz, "Effect of Heat Treatment on the Elemental Distribution of Si,C,N,O Fibers," Ceramics International, **18**, 271-277, (1992).

31) A. L. Peterson, R. E Jones, and E.C. Pudnos, "Properties of Textile Grade Ceramic Fibers," 24th Int. SAMPE Tech. Conf. Proc. T992-T-1004, (1992).

32) D-D. Lee, S-J. Kang, G. Petsow, and D. N. Yoon, "Effect of Alpha to Beta (Beta') Phase Transition on the Sintering of Silicon Nitride Ceramics," J. Am. Ceram. Soc., **73** [3] 767-769 (1990).

33) H. Wada, M-J. Wang, and T-Y Tien, "Stability of Phases in the Si-C-N-O System," J. Am. Ceram. Soc., **71** [10] 837-840 (1988).

34) G. B. Freeman, R. L Starr, J. N. Harris, R. E. Kirchain, and D. L. Mohr, "Characterization of the Fiber-Matrix Interfaces in a Silicon Carbide-Silicon Nitride Ceramic Composite System," Heat-Resistant Mater. Proc. Int. Conf., 299-306, (1991).

35) B. Budianski, J.W. Hutchinson, and A.G. Evans, "Matrix Fracture in Fiber-Reinforced Ceramics," Journal of Mechanical and Physical Solids, **34**, 167-189, (1986).

36) C. H. Hsueh, "Toughening Behavior and Inerfacial Properties of Fiber-Reinforced Ceramic Composites," Journal of Energy Resources Technology, **113** [3] 197-203 (1991).

37) R. H. Jones, N.T. Saenz, and C.H. Schilling, "Interfacial Chemistry and Structure in Ceramic Composites," Report for the U.S. Department of Energy, Report # DE91-005676, September, (1990).

38) L.F. Albright and T. C-H. Tsai, "Importance of Surface Reactions in Pyrolysis Units," Pyrolysis: Theory and Industrial Practice, Academic Press, London, 233-254, (1983).

39) A.I. Lacava, E.D. Fernandez-Raone, and M. Caraballo, "Mechanism of Surface Carbon Formation During the Pyrolysis of Benzene in the Presence of Hydrogen," ACS Symposium Series 202, Ch. 6, 109-121, (1982).

40) L.F. Albright and J.C. Marek, "Coke Formation During Pyrolysis: Roles of Residence Time, reactor Geometry, and Time of Operation," Ind. Eng. Chem. Res., **27** [5] 743-751 (1988).

41) R.T.K. Baker and P.S. Harris, "The Formation of Filamentous Carbon," Chemistry and Physics of Carbon, Marcel Dekker, New York, Vol. 14, Ch. 2, 83-165, (1978).

42) M.J. Graff and L.F. Albright, "Coke Deposition From Acetylene, Butadiene and Benzene Decompositions at 500-900C on Solid Surfaces," Carbon, **20** [4] 319-330 (1982).

43) "Ceramics in Heat Exchangers," Ed. B.D. Foster and J. B. Patton, Advances in Ceramics, The American Ceramic Society, Westerville, OH, [14], (1985).